Chemistry–A European Journal

Supporting Information

Hydride-Containing Pt-doped Cu-rich Nanoclusters: Synthesis, Structure, and Electrocatalytic Hydrogen Evolution

Rhone P. Brocha Silalahi, Hao Liang, Yongsung Jo, Jian-Hong Liao, Tzu-Hao Chiu, Ying-Yann Wu, Xiaoping Wang, Samia Kahlal, Qi Wang, Woojun Choi, Dongil Lee,* Jean-Yves Saillard,* and C. W. Liu*

Chemistry—A European Journal

Supplementary Information

Hydride-Containing Pt-doped Cu-rich Nanoclusters: Synthesis, Structure, and Electrocatalytic Hydrogen Evolution

Rhone P. Brocha Silalahi,[a] Hao Liang,[b] Yongsung Jo,[c] Jian-Hong Liao,[a] Tzu-Hao Chiu,[a] Ying-Yann Wu,[a] Xiaoping Wang,[d] Samia Kahlal,[b] Qi Wang,[b] Woojun Choi,[c] Dongil Lee,*[c] Jean-Yves,*[b] and C. W. Liu*[a]

Experimental section

Materials and Measurement

All the reactions were carried out under an N_2 atmosphere using the standard Schlenk technique. The solvents used in this work were distilled before use, following standard protocols. All chemicals were purchased from different commercial sources available and used as received. $[Cu_{20}H_{11}\{S_2P(O^iPr)_2\}_9]$,[1] $[Pt\{S_2P(O^iPr)_2\}_2]$,[2] and $[Cu_{11}H_2\{S_2P(O^iPr)_2\}_6(CCPh)_3]$,[3] were prepared by following the procedures reported in the literature. NMR spectra were recorded on a Bruker Advance DPX300 FT-NMR spectrometer that operates at 400 MHz while recording ^1H, 121.5 MHz for ^{31}P, 46.1 MHz for ^2H. Used residual solvent proton references: δ, $CDCl_3$, 7.26 and δ, d_6-acetone, 2.10. The $^{31}P\{^1H\}$ NMR spectra were referenced to external 85% H_3PO_4 at δ = 0.00 ppm. The chemical shift (*δ*) and coupling constants (J) are reported in ppm and Hz. ESI-mass spectra were recorded on a Fison Quattro Bio-Q (Fisons Instruments, V.G. Biotech, U. K.). UV–Visible absorption spectra were measured on a Perkin Elmer Lambda 750 spectrophotometer using quartz cells with a path length of 1 cm.

Synthesis of $[PtH_2Cu_{14}\{S_2P(O^iPr)_2\}_6(CCPh)_6]$ (1)

Method A: In a flame-dried Schlenk tube, $[Cu_{20}H_{11}\{S_2P(O^iPr)_2\}_9]$ (0.1 g, 0.031 mmol) and $[Pt\{S_2P(O^iPr)_2\}_2]$ (0.019 g, 0.031 mmol) were suspended in THF (5 mL) along with phenylacetylene (40 µL, 0.281 mmol). The resulting mixture was stirred at ambient temperature for 48 hours under N_2 conditions. The solvent was evaporated under the vacuum. The obtained powder was washed with water, extracted in diethyl ether, and evaporated under vacuum. The precipitates were washed with methanol (3x5 mL) to remove the ligand impurities. The residue was extracted in dichloromethane and filtered through aluminium oxide. Finally, the solvent was evaporated to dryness under vacuum to get a dark purple precipitate of $[PtH_2Cu_{14}\{S_2P(O^iPr)_2\}_6(CCPh)_6]$ (**1**). The yield obtained was 0.0028 g, 14.97% based on Cu.

Similarly, deuterium analogues of $[PtD_2Cu_{14}\{S_2P(O^iPr)_2\}_6(CCPh)_6]$ (**1D**) (0.0029 g, 15.77% based on Cu) were synthesis by using $[Cu_{20}D_{11}\{S_2P(O^iPr)_2\}_9]$ (0.1 g; 0.031 mmol) in place of $[Cu_{20}H_{11}\{S_2P(O^iPr)_2\}_9]$.

Method B: In a flame-dried Schlenk tube $[Cu_{11}H_2\{S_2P(O^iPr)_2\}_6(CCPh)_3]$ (0.05 g; 0.0219 mmol) were added along with 10 mL THF; then $[Pt\{S_2P(O^iPr)_2\}_2]$ (0.013 g; 0.0219 mmol) were added under vigorous stirring. The reaction was stirred for 4 hours under an N_2 atmosphere at room temperature. The solvent was evaporated under the vacuum, and the residue was washed with methanol. The dark purple precipitate was collected in CH_2Cl_2 and evaporated to dryness under the vacuum to get a pure dark purple powder of **1**. The yield of **1** was obtained in 11% based on Cu.

Method C: In a flame-dried Schlenk tube, $[NH_4][S_2P\{O^iPr\}_2]$ (0.027 g, 0.15 mmol) and phenylacetylene (40 µL, 0.15 mmol) were suspended in THF (30 cm^3), and addition of $[Cu(CH_3CN)_4](PF_6)$ (0.13 g, 0.35 mmol) and triethylamine (41 µL, 0.3 mmol) took place. After the mixture was stirred for 5 min, the $[Pt\{S_2P(O^nPr)_2\}_2]$ (0.03g, 0.05 mmol) and $NaBH_4$ (0.0037 g, 0.1 mmol) was added to the mixture. The resulting mixture was stirred at 0°C for 6 hours. The solvent was evaporated under vacuum, and the residue was dissolved in DCM and washed with water (3 × 15 mL). After separation, the organic layer was passed through Al_2O_3, and the purple solution was collected. The solvent was evaporated under the vacuum, and the precipitate was washed with methanol (3 × 15 mL) to remove [Cu7H{S2P(OiPr)2}6] and ligand impurities. Finally, the solvent was evaporated to dryness under vacuum to obtain the pure dark purple powder of **1**. The yield of **1** was obtained in 17% based on Cu.

[$\mathbf{1_H}$]: ESI-MS: *m/z* 2971.31 Da (calcd. *m/z* 2970.33 Da) for $([PtH_2Cu_{14}\{S_2P(O^iPr)_2\}_6(CCPh)_6]+H^+)^+$. ^{1}H NMR (400 MHz, $CDCl_3$): 7.70 (m, 12H, $C_6\mathit{H}_5$), 7.22 (18H, $C_6\mathit{H}_5$), 5.15 (6H, OC*H*), 4.67 (6H, OC*H*), 1.30 (32H, CH_3), 1.12 (16H, CH_3), 0.97 (16H, CH_3), 0.50 (2H, μ_4-*H,* $J_{Pt\text{-}H}$=712 Hz) ppm; ^{31}P NMR (121. MHz, d_6-acetone): 102.54 ppm. ^{13}C NMR (100.6 MHz, $CDCl_3$): 131.98, 127.72, 126.97, 125.28, 92.69, 77.29, 73.79, 23.45 ppm. FT-IR (cm^{-1}): 2974.1, 2932.9, 2870.5, 1968.2, 1730.6, 1592.7, 1483.0, 1176.9, 1069.3, 972.1, 814.6, 753.7, and 688.9 . Elem. Anal.: C: 32.01% and H: 3.73% (calcd.: C: 33.93%, and H: 3.93%).

[$\mathbf{1_D}$]: ESI-MS: *m/z* 2973.41 Da (calcd. *m/z* 2973.35 Da) for $([PtD_2Cu_{14}\{S_2P(O^iPr)_2\}_6(CCPh)_6]+H^+)^+$. ^{1}H NMR (400 MHz, $CDCl_3$): 7.66 (12H, $C_6\mathit{H}_5$),

7.20 (18H, C_6H_5), 5.09 (6H, OC*H*), 4.82 (6H, OC*H*), 1.35 (32H, CH_3), 1.08 (16H, CH_3), 0.94 (16H, CH_3) ppm; ^{2}H NMR (400 MHz, $CHCl_3$): 0.49 (2D, μ_4-*D*) ppm; ^{31}P NMR (400 MHz, $CDCl_3$): 101.3 ppm.

Synthesis of [PtHCu$_{11}${S$_2$P(O^{i}Pr)$_2$}$_6$(CCPh)$_4$] (2) and PtHCu$_{11}${S$_2$P(O^{i}Pr)$_2$}$_6$(CCPh)$_3$] (3)
In a flame-dried Schlenk tube [PtH$_2$Cu$_{14}${S$_2$P(O^{i}Pr)$_2$}$_6$(CCPh)$_6$] (**2**) (0.1 g; 0.035 mmol) were added to a flask along with 5 mL acetone solvent; then two equiv. CF_3COOH (5.0 µL; 0.07 mmol) was added under vigorous stirring. The reaction was stirred for 10 minutes under an N_2 atmosphere at room temperature. The solvent was evaporated under vacuum, and the residue was washed with CH_2Cl_2/water. The organic layer separated and passed through Al_2O_3. The organic layer was collected and dried under the vacuum. The residue was washed with methanol to separate clusters **2** and **3**. The MeOH layer was collected and dried to get the orange precipitate of cluster **2**. The remaining residue was extracted in dichloromethane and dried to get the red powder of **3**. The yield of cluster **2** is 19 % based on Cu, and cluster **3** is a 12 % yield (based on Cu).

Similarly, deuterium analogues of [PtDCu$_{11}${S$_2$P(O^{i}Pr)$_2$}$_6$(CCPh)$_4$] (**2$_D$**) (16 % based on Cu) and [PtD$_2$Cu$_{11}${S$_2$P(O^{i}Pr)$_2$}$_6$(CCPh)$_3$] (**3$_D$**) (11 % based on Cu) was synthesis by using [PtD$_2$Cu$_{14}${S$_2$P(O^{i}Pr)$_2$}$_6$(CCPh)$_6$] (0.1 g; 0.031 mmol) in place of [PtH$_2$Cu$_{14}${S$_2$P(O^{i}Pr)$_2$}$_6$(CCPh)$_6$].

[2$_H$]: ESI-MS: *m/z* 2642.42 Da (calcd. *m/z* 2641.38 da) for [PtHCu$_{11}${S$_2$P(O^{i}Pr)$_2$}$_6$(CCPh)$_4$+Cu$^+$]$^+$. ^{1}H NMR (400 MHz, *d$_6$*-acetone): 7.39-7.56 (20 H, -*C$_6$H$_5$*), 4.88-4.92 (12 H, *CH*), 4.45 (1H, μ_4-H) ($J_{Pt\text{-}H}$=880 Hz), 1.42 - 1.44 (72 H, *CH$_3$*) ppm. ^{31}P NMR (121.49 MHz, *d$_6$*-acetone): 93.4, 96.5, 98.1, 100.4, and 102.2 ppm. Elem. Anal.: C: 30.67% and H: 4.69% (calcd. C: 31.67%, and H: 4.10%).

[2$_D$]: ESI-MS: *m/z* 2643.40 Da (calcd. *m/z* 2643.38 Da) for ([PtDCu$_{11}${S$_2$P(O^{i}Pr)$_2$}$_6$(CCPh)$_4$+Cu$^+$]$^+$. ^{1}H NMR (400 MHz, *d$_6$*-$CDCl_3$): 7.25-7.68 (20 H, -*C$_6$H$_5$*), 4.89-4.85 (12 H, *CH*), 1.08 - 1.44 (72 H, *CH$_3$*) ppm. ^{31}P NMR (121.49 MHz, $CDCl_3$): 102.3, 99.9, 98.3, 97.1, 95.2 and 92.2 ppm.

[**3**$_{H}$]; ESI-MS: ESI-MS: *m/z* 2477.41 (calcd. 2477.43) for $[PtH_2Cu_{11}\{S_2P(O^iPr)_2\}_6(CCPh)_3+H^+]^+$. ^{1}H NMR (600 MHz, d_6-$CDCl_3$): 7.20-7.61 (15 H, -C_6H_5), 4.79-4.26 (12 H, *CH*), 2.35 (2H, μ_4-H) (J_{Pt-H}= 732 Hz), 1.22-1.38 (72 H, CH_3) ppm. ^{31}P NMR (121.49 MHz, $CDCl_3$): 100.18 ppm. Elem. Anal.: C: 28.78 %, S: 15.09 %, and H: 3.96 %. (calcd. C: 29.07 %, S: 15.52 % and H: 4.11 %).

[**3**$_{D}$]; ESI-MS: ESI-MS: *m/z* 2543.99 Da (calcd. *m/z* 2543.36 Da) for $[PtD_2Cu_{11}\{S_2P(O^iPr)_2\}_6(CCPh)_3+Cu^+]^+$. ^{1}H NMR (400 MHz, d_6-$CDCl_3$): 7.21-7.62 (15 H, -C_6H_5), 4.81-5.26 (12 H, *CH*), 0.80-1.37 (72 H, CH_3) ppm. ^{31}P NMR (121.49 MHz, $CDCl_3$): 100.18 ppm. ^{2}H NMR (400 MHz, $CHCl_3$): 2.448 (2D, μ_4-*D*) ppm.

Preparation of [2]$_2$·[4]$_{0.85}$·[5]$_{0.15}$ and [3]$_2$·[4]$_{0.75}$·[5]$_{0.25}$

Because of the difficulty in obtaining crystals [**2**] and [**3**] after purifications, we try to grow single crystals directly while the reaction is still taking place. In a test tube, $[PtH_2Cu_{14}\{S_2P(O^iPr)_2\}_6(CCPh)_6]$ (**1**) (0.1 g; 0.035 mmol) was added to a flask along with 5 mL CH_2Cl_2 solvent, followed by the addition of two equiv. CF_3COOH (5.0 µL; 0.070 mmol). The solution was subjected to the diffusion of n-hexane to afford dark-red **[2]$_2$·[4]$_{0.85}$·[5]$_{0.15}$** and dark-orange**[3]$_2$·[4]$_{0.75}$·[5]$_{0.25}$** crystals after 4 weeks. After so many attempts, the co-crystals of **[2]$_2$·[4]$_{0.85}$·[5]$_{0.15}$** and **[3]$_2$·[4]$_{0.75}$·[5]$_{0.25}$** were finally obtained from two separate test tubes. The formation of [**4**] and [**5**] is due to decomposition reactions. The presence of chloride in clusters [**4**] and [**5**] most likely originating from the chloro-solvent used for crystallization.

Single-Crystal X-ray Crystallography

Single crystals of **1**, ([**2**]$_2$[**4**]$_{0.85}$[**5**]$_{0.15}$)**,** and **(**[**3**]$_2$[**4**]$_{0.75}$[**5**]$_{0.25}$**)** were mounted on the tip of glass fiber coated with paratone oil and then frozen. Data were collected on a Bruker APEX II CCD diffractometer using graphite monochromated Mo Kα radiation (λ = 0.71073 Å) at 100 K. Absorption corrections for the area detector were performed SADABS,[4] and the integration of raw data frame was performed with SAINT.[5] The structure was solved by direct methods and refined by least-squares against F^2 using the SHELXL-2018/3 package[6,7] incorporated in SHELXTL/PC V6.14.[8] All non-hydrogen atoms were refined

anisotropically. The structure reported herein has been deposited at the Cambridge Crystallographic Data Centre, CCDC no. 2296486 (**1**), 2296488 ([**2**]$_2$[**4**]$_{0.85}$[**5**]$_{0.15}$), and 2296489 ([**3**]$_2$[**4**]$_{0.75}$[**5**]$_{0.25}$).

Single-Crystal Neutron Diffraction

The location of hydrides in **1$_N$** was confirmed through a single-crystal neutron diffraction experiment conducted at ORNL's Spallation Neutron Source using the TOPAZ single-crystal neutron time-of-flight (TOF) Laue diffractometer.[9]. A black block-shaped crystal (0.69 mm × 1.95 mm × 2.05 mm) was attached to a MiTeGen loop using a perfluorinated grease (Krytox GPL 205) and transferred to TOPAZ goniometer for data collection at 100 K. A total of 28 crystal orientations optimized with CrystalPlan software[10] were used to ensure better than 95% coverage of a hemisphere of reciprocal space. Each orientation was measured for approximately 4 h. Raw peaks intensities were obtained using the 3-D ellipsoidal Q-space integration method available in Mantid.[11] Data normalization, including Lorentz, neutron TOF spectrum, and detector efficiency corrections, were carried out with the ANVRED3 program.[12] A Gaussian numerical absorption correction was applied with $\mu = 1.1544 + 0.8547\ \lambda\ cm^{-1}$. The reduced data were saved in SHELX HKLF2 format, in which the neutron wavelength for each reflection was recorded separately. Non-hydrogen atom positions in the X-ray structure were used for the initial refinement of the neutron structure. Hydrogen atoms on carbon atoms are placed using the riding model available in SHELXL-2018.[13] The two hydrides in **1$_N$** were located from the difference Fourier map calculated using the neutron data. All atoms, including H, were refined anisotropically, and the neutron structure was then refined successfully to convergence using the SHELXL-2018 program. Selected crystallographic data and distances are listed in Tables 1 and Supplementary Table 1. The structure reported herein has been deposited at the Cambridge Crystallographic Data Centre, CCDC no. 2296487.

Electrochemical measurements

Linear sweep voltammograms (LSVs) were obtained on an electrochemical workstation (ZIVE BP2, WonATech) in a three-electrode electrochemical cell consisting of a cluster-immobilized carbon paper, a Pt foil anode (3 cm^2), and an Ag/AgCl (1.0 M KCl) reference

electrode. The working electrodes were fabricated by dropcasting a catalyst solution (in 1:1 CH_2Cl_2-acetone) onto a carbon paper (1 cm^2, Avcarb - MGL190) with a typical loading of 2.5 nmol cm^{-2}. For comparison, a benchmark Pt/C (20 wt% Pt on VC-72, Premetek) electrode was prepared by dropcasting 200 µL of a catalyst ink, made by dispersing 10 mg of Pt/C with 200 µL of Nafion solution (5 wt%, Sigma-Aldrich) in 800 µL of isopropyl alcohol, onto the carbon paper (2 mg cm^{-2}). The electrolyte solution of 0.5 M H_2SO_4 was degassed with high-purity Ar for 30 min. Electrode potentials measured on the Ag/AgCl scale ($E_{Ag/AgCl}$) were converted to the RHE scale (E_{RHE}) using the following equation:

$$E_{RHE} = E_{Ag/AgCl} + 0.235 + 0.059\ pH \quad (1)$$

Constant potential electrolysis was conducted in an H-cell constructed by compressing two glass compartments under vigorous stirring. One region of the H-cell was used for the cathodic reaction, in which the prepared working electrode (PtH_2Cu_{14}/C **(1)**, $PtHCu_{11}$/C **(2)** or PtH_2Cu_{11}/C **(3)**) and reference electrode (Ag/AgCl) were immersed in 60 mL of a degassed electrolyte solution of 0.5 M H_2SO_4. The other region in the H-cell was used for the anodic reaction and contained 60 mL of the same electrolyte solution; a Pt foil anode was dipped into the solution. The two compartments were separated by a Nafion 117 membrane (Dupont). The gaseous products were analyzed using gas chromatography (Agilent, GC 7820A) equipped with a thermal conductivity detector (TCD). The turnover frequency (TOF) and faradaic efficiency (FE) for HER were determined as follows:

$$\text{TOF } (s^{-1}) = \frac{\text{produced } H_2 \text{ (mol)}}{\text{amount of catalyst (mol)} \times \text{time (s)}} \quad (2)$$

$$\text{FE } (\%) = \frac{\text{produced } H_2 \text{ (mol) x } 2 \times \text{Faraday constant } (96485\ C/mol)}{\text{total charge consumed (C)}} \times 100 \quad (3)$$

Square wave voltammetry (SWV) of 1.0 mM Pt-Cu NCs was conducted in CH_2Cl_2 containing 0.1 M Bu_4NPF_6. Voltammograms were obtained using a Pt disk working electrode, Pt wire counter electrode and $Ag/AgNO_3$ reference electrode. The potentials

were calibrated using ferrocene ($Fc^{+/0}$) as an internal standard.

Computational Details

Density Functional Theory (DFT) calculations were carried out using the Gaussian (R) 16 program.[14] The valence triple-zeta polarization functions (def2-TZVP) basis set was used,[15] together with the Perdew-Burke-Ernzerhof (PBE0)[16,17] functional. All the optimized structures were confirmed as true minima on their potential energy surface by analytical vibration frequency calculations. Natural atomic orbital (NAO) populations and Wiberg bond indices were computed with the natural bond orbital NBO 6.0 program[18-20] implemented in the Gaussian (R) 16 package. The UV-visible transitions were calculated by means of time-dependent-DFT (TD-DFT) calculations.[21] Only singlet-singlet, *i.e.* spin-allowed, transitions were computed. The UV–visible spectra were simulated from the computed TD-DFT transitions and their oscillator strengths by using the Multiwfn program,[22] each transition being associated with a Gaussian function of half-height width equal to 3000 cm^{-1}.

References

[1] R. S. Dhayal, J.-H. Liao, X. Wang, Y.-C. Liu, M.-H. Chiang, S. Kahlal, J.-Y. Saillard, C. W. Liu, *Angew. Chem. Int. Ed*. **2015**, *54*, 13604-13608.

[2] M. Gianini, W. R. Caseri, V. Gramlich, U. W. Suter, *Inorg. Chim. Acta.* **2000**, *299*, 199-208.

[3] R. P. B. Silalahi, G.-R. Huang, J.-H. Liao, T.-H. Chiu, K. K. Chakrahari, X. Wang, J. Cartron, S. Kahlal, J.-Y. Saillard, C. W. Liu, *Inorg. Chem*. **2020**, *59*, 2536-2547.

[4] G. M. Sheldrick, *SADABS, version 2014-11.0. Bruker area detector absorption corrections*, Bruker AXS Inc., Madison, WI, **2014**.

[5] G. M. Sheldrick, *SAINT, v4.043. Software for the CCD detector system*, Siemens Analytical Instruments Madison, WI, *1995*.

[6] G. M. Sheldrick, *Acta Crystallogr., Sect. A: Found. Crystallogr.* **2008**, *A64*, 112– 122.

[7] T. Gruene, H. W. Hahn, A. V. Luebben, F. Meilleur, G. M. Sheldrick, *J. Appl. Crystallogr.* **2014**, *47*, 462– 466.

[8] G. M. Sheldrick, *SHELXTL, version 6.14 (PC version) Program Library for Structure Solution and Molecular Graphics*, Bruker Analytical X-ray Systems, Madison, Wisconsin, USA, **2003**.

[9] Z.-L. Xue, A. J. Ramirez-Cuesta, C. M. Brown, S. Calder, H. Cao, B. C. Chakoumakos, L. K. Daemen, A. Huq, A. I. Kolesnikov, E. Mamontov, A. A. Podlesnyak, X. Wang, *Eur. J. Inorg. Chem.* **2019**, *8*, 1065–1089.

[10] J. Zikovsky, P. F. Peterson, X. P. Wang, M. Frost, C. M. Hoffmann, *J. Appl. Crystallogr.* **2011**, *44*, 418-423.

[11] A. J. Schultz, M. R. V. Jørgensen, X. Wang, R. L. Mikkelson, D. J. Mikkelson, V. E. Lynch, P. F. Peterson, M. L. Green, C. M. Hoffmann. *Appl. Crystallogr.* **2014**, *47*, 915–921.

[12] A. J. Schultz, K. Srinivasan, R. G. Teller, J. M. Williams, C. M. Lukehart, *J. Am. Chem. Soc.* **1984**, 106, 999–1003.

[13] G. M. Sheldrick, *Acta Crystallogr. Sect. C: Struct. Chem.* **2015**, *C71*, 3-8.

[14] M. J. Frisch, G. W. Trucks, H. B. Schlegel, G. E. Scuseria, M. A. Robb, J. R. Cheeseman, G. Scalmani, V. Barone, G. A. Petersson, H. Nakatsuji, X. Li, M. Caricato, A. V. Marenich, J. Bloino, B. G. Janesko, R. Gomperts, B. Mennucci, H. P. Hratchian, J. V. Ortiz, A. F. Izmaylov, J. L. Sonnenberg, D. Williams-Young, F. Ding, F. Lipparini, F. Egidi, J. Goings, B. Peng, A. Petrone, T. Henderson, D. Ranasinghe, V. G. Zakrzewski, J. Gao, N. Rega, G. Zheng, W. Liang, M. Hada, M. Ehara, K. Toyota, R. Fukuda, J. Hasegawa, M. Ishida, T. Nakajima, Y. Honda, O. Kitao, H. Nakai, T. Vreven, K. Throssell, J. A. Montgomery Jr., J. E. Peralta, F. Ogliaro, M. J. Bearpark, J. J. Heyd, E. N. Brothers, K. N. Kudin, V. N. Staroverov, T. A. Keith, R. Kobayashi, J. Normand, K. Raghavachari, A. P. Rendell, J. C. Burant, S. S. Iyengar, J. Tomasi, M. Cossi, J. M. Millam, M. Klene, C. Adamo, R. Cammi, J. W. Ochterski, R. L. Martin, K. Morokuma, O. Farkas, J. B. Foresman, D. J. Fox, *Gaussian 16, Revision C.01*, Gaussian, Inc., Wallingford CT, **2016**.

[15] F. Weigend, R. Ahlrichs, *Phys. Chem. Chem. Phys.* **2005***, 7*, 3297-3305.

[16] J. P. Perdew, M. Ernzerhof, K. Burke, *J. Chem. Phys*. **1996**, *105*, 9982–9985.

[17] C. Adamo, V. Barone, *Chem. Phys.* **1999**, *110,* 6158–6170.

[18] A. E. Reed, F. Weinhold, *J. Chem. Phys*. **1983**, *78*, 4066-4073.

[19] J. E. Carpenter, F. Weinhold, *J. Mol. Struct. (Theochem*). **1988**, *169*, 41-62.

[20] A. E. Reed, L. A. Curtiss, F. Weinhold, *Chem. Rev*. **1988**, *88*, 899-926.

[21] C. A. Ullrich, *Time-Dependent Density-Functional Theory, Concepts and Applications*, Oxford University Press, **2012**.

[22] T. Lu, F. A. Chen, *J. Comput. Chem*. **2012**, *33*, 580-592.

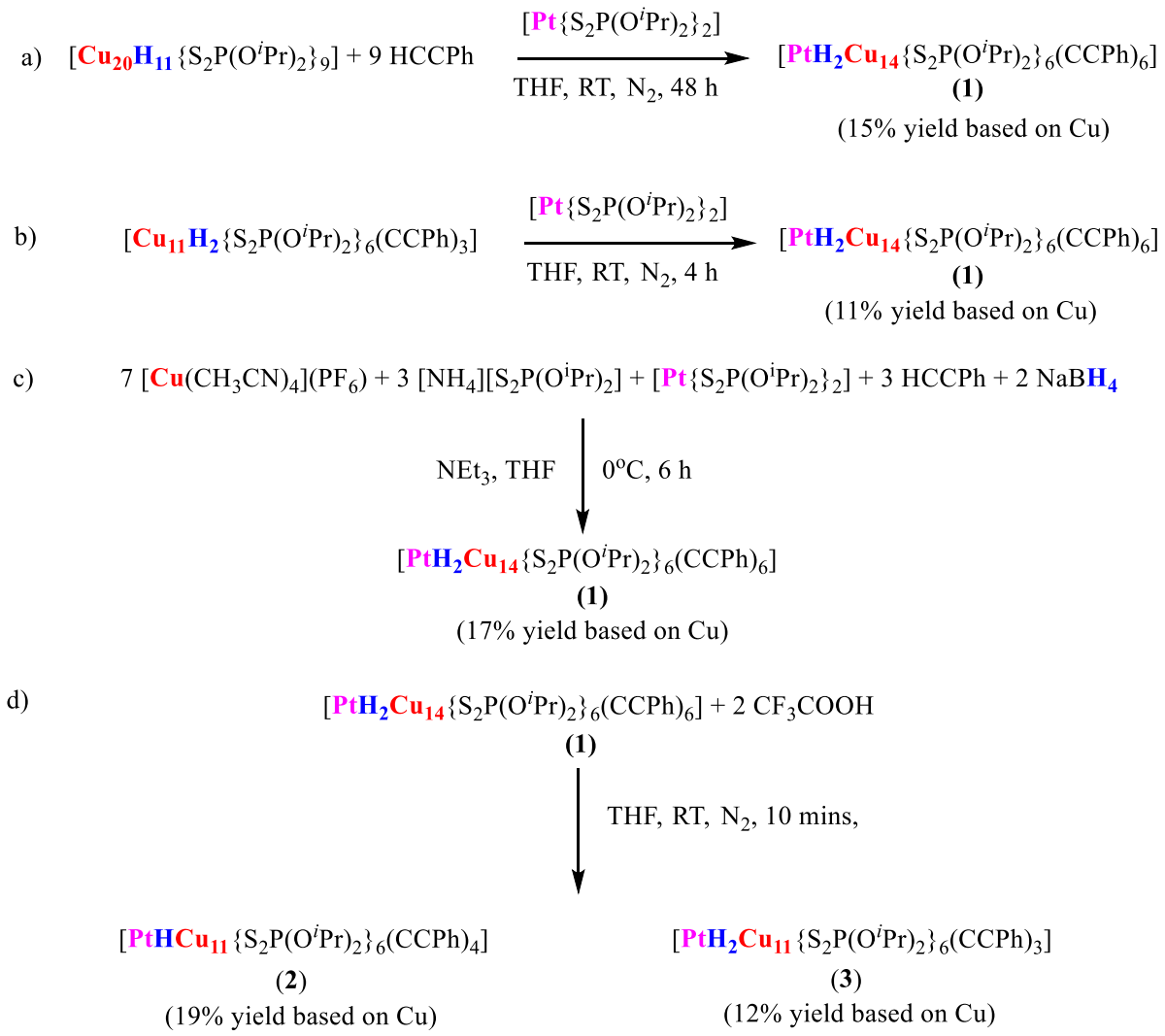

Scheme S1. The general synthesis of Pt-doped Cu-rich hydride clusters by using copper hydride precursors, a) $[Cu_{20}H_{11}\{S_2P(O^iPr)_2\}_9]$ and b) $[Cu_{11}H_2\{S_2P(O^iPr)_2\}_6(CCPh)_3]$, c) one-pot method, and d) reaction with CF_3COOH.

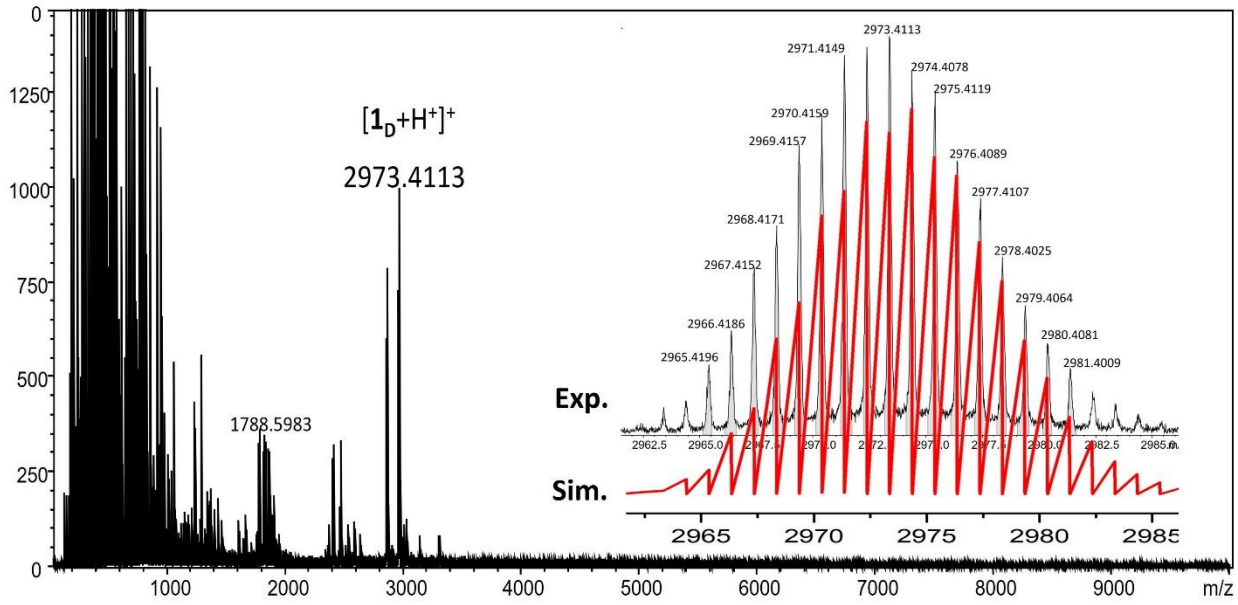

Figure S1. Positive ESI-MS spectrum of the [**1**$_D$+H$^+$]$^+$ cluster. The inset shows the isotope pattern of the experimental one at the top and the simulation at the bottom.

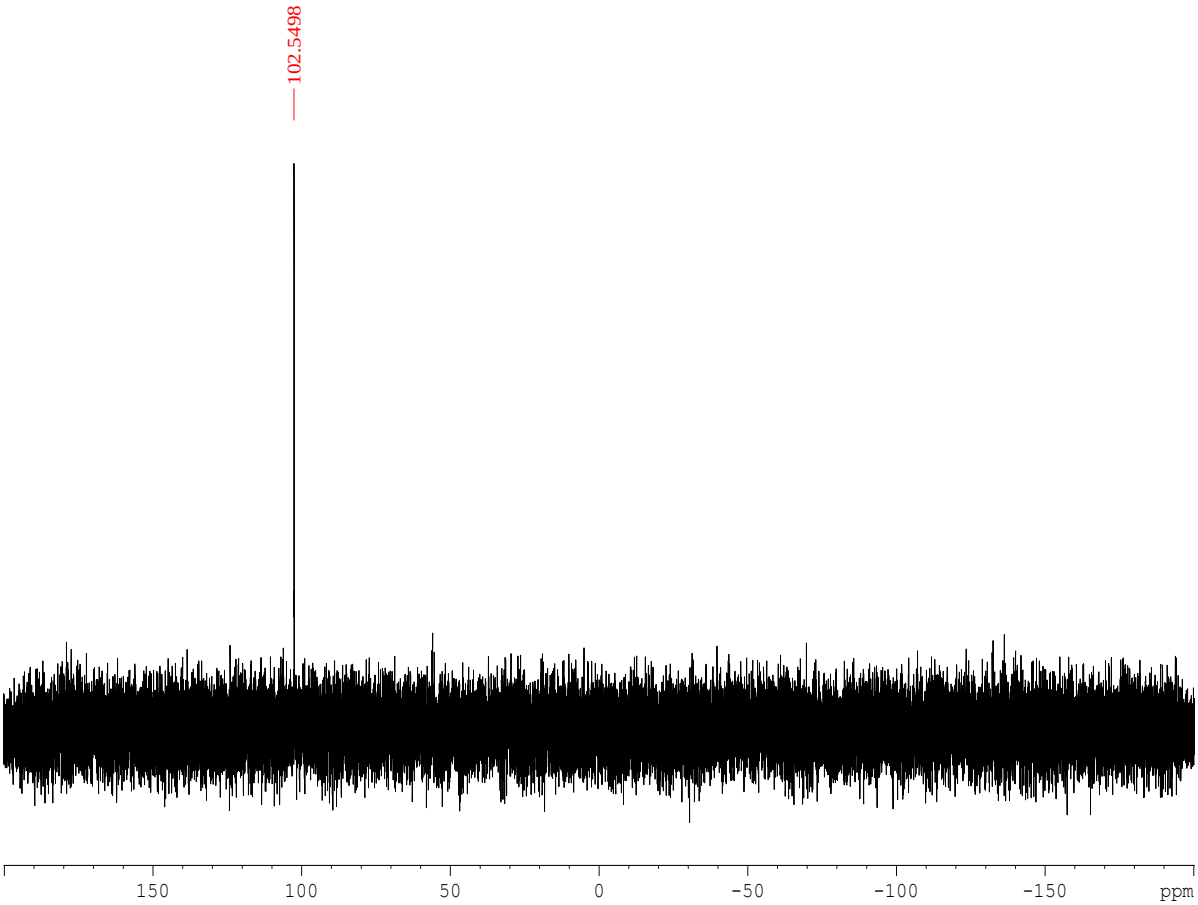

Figure S2. The $^{31}P\{^{1}H\}$ NMR spectrum of cluster **1** in $CDCl_3$.

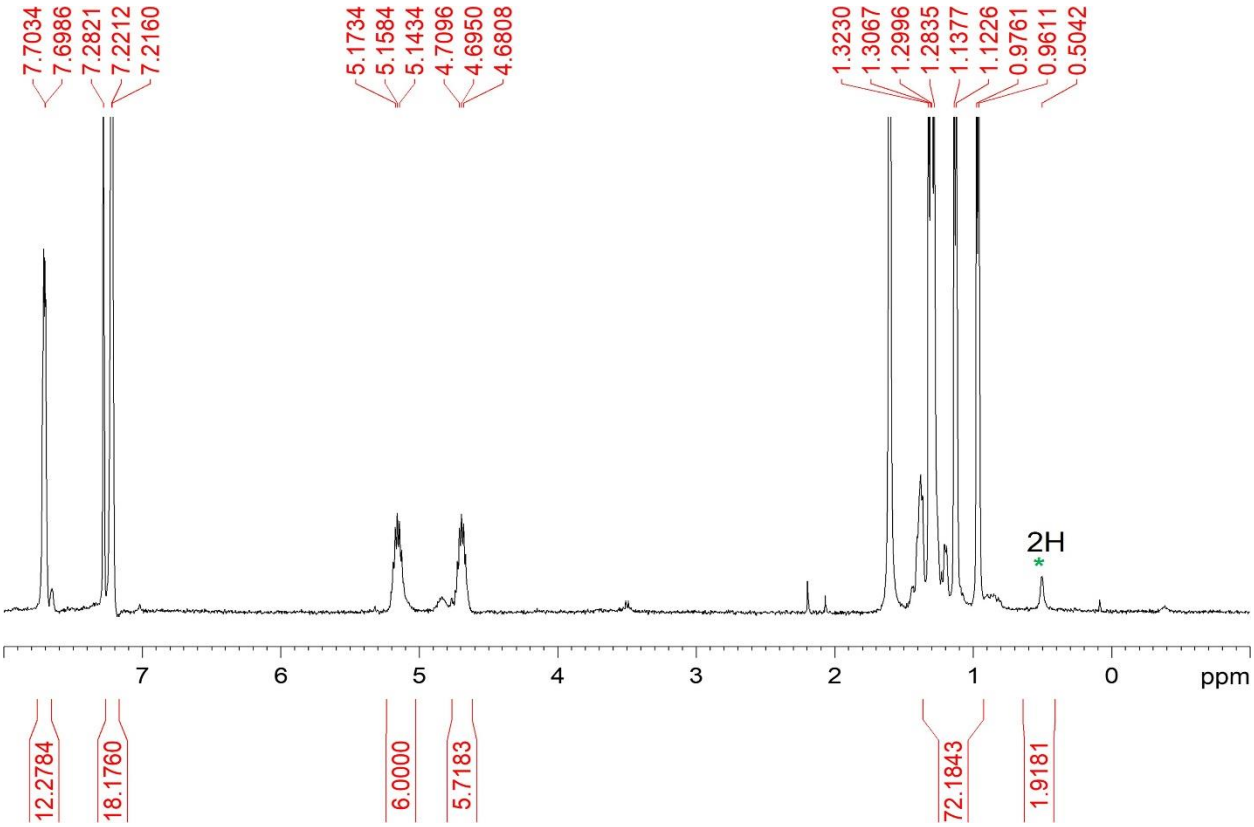

Figure S3. The ^{1}H NMR spectrum of **1** in $CDCl_3$.

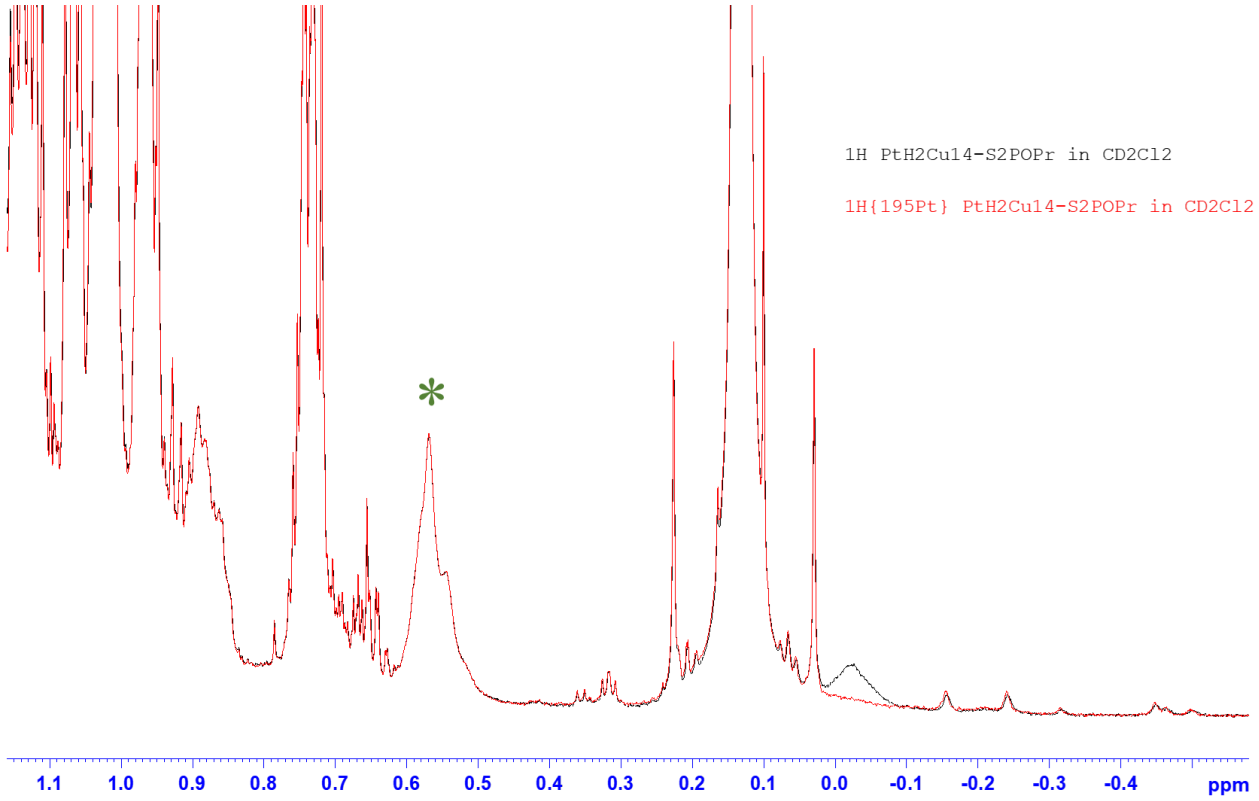

Figure S4. The $^{1}H\{^{195}Pt\}$ NMR experimental (black) and simulation (red) spectrum of cluster **1** in CD_2Cl_2.

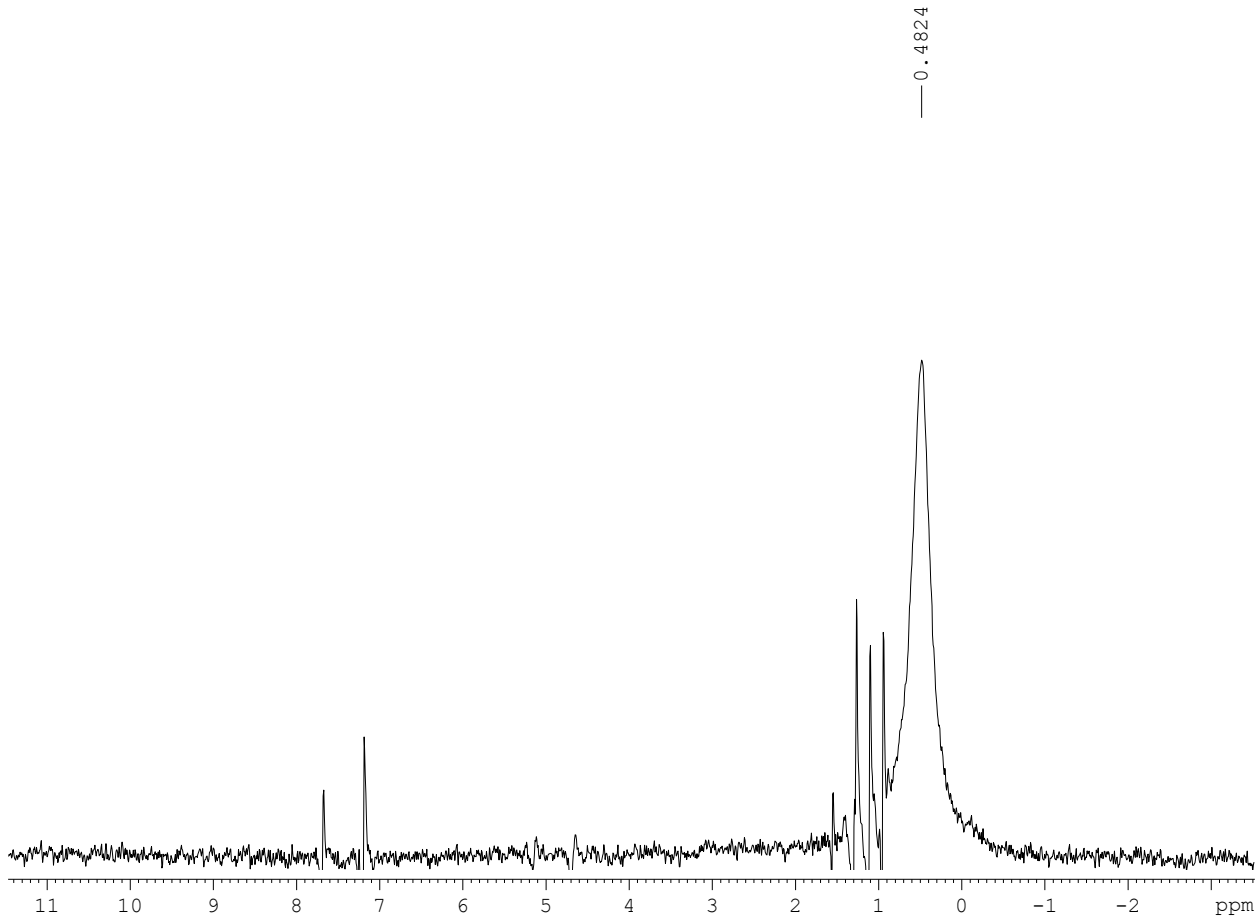

Figure S5. The $^{1}H\{^{195}Pt\}$ 1D-HMQC with decoupling spectrum of cluster **1** in $CDCl_3$.

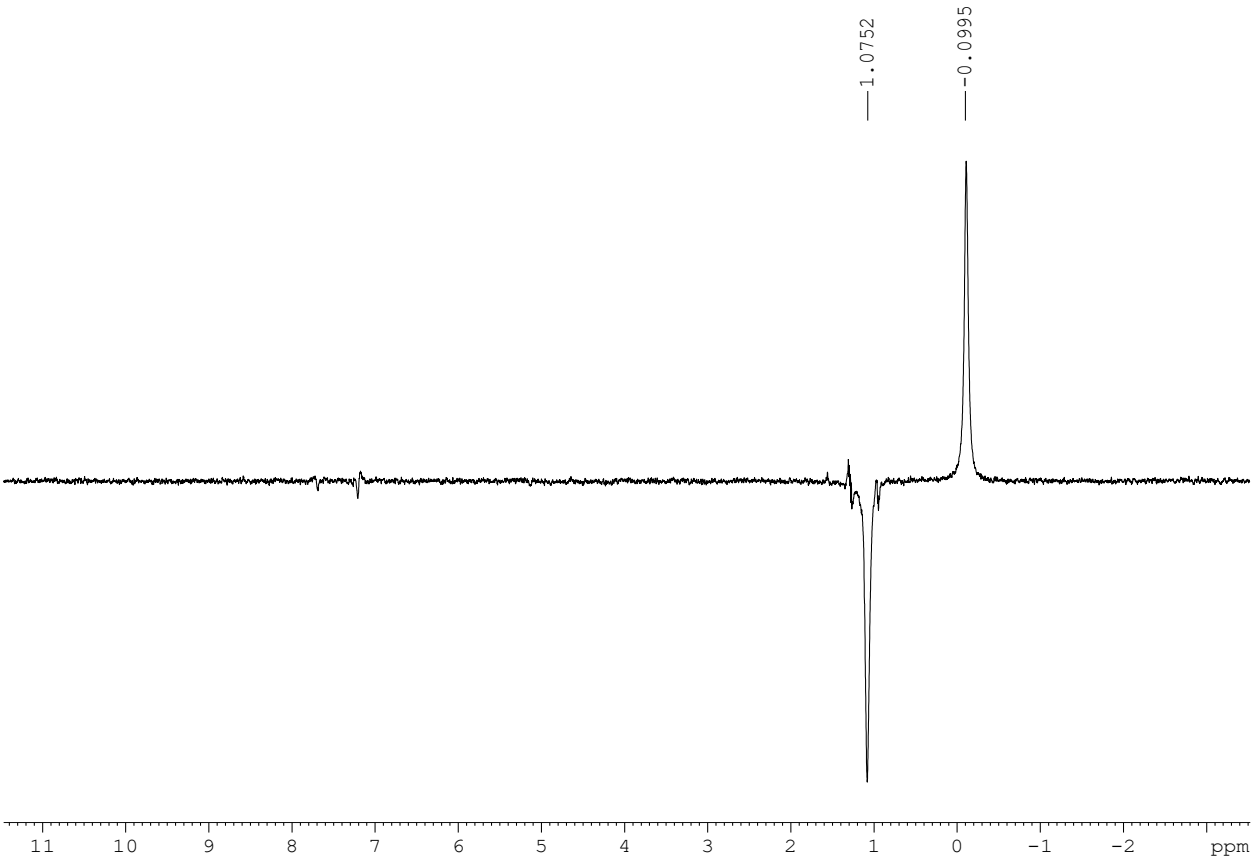

Figure S6. The $^{1}H\{^{195}Pt\}$ 1D-HMQC without decoupling spectrum of cluster **1** in $CDCl_3$.

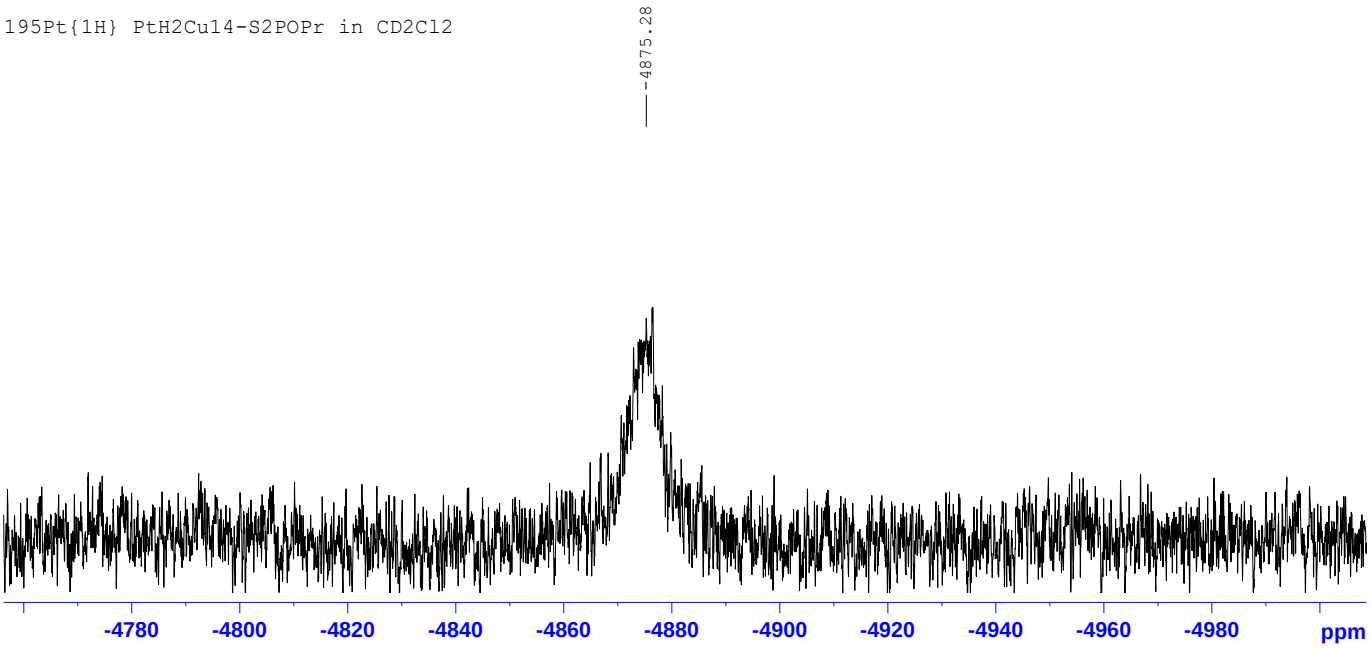

Figure S7. The $^{195}Pt\{^{1}H\}$ NMR spectrum of cluster **1** in CD_2Cl_2.

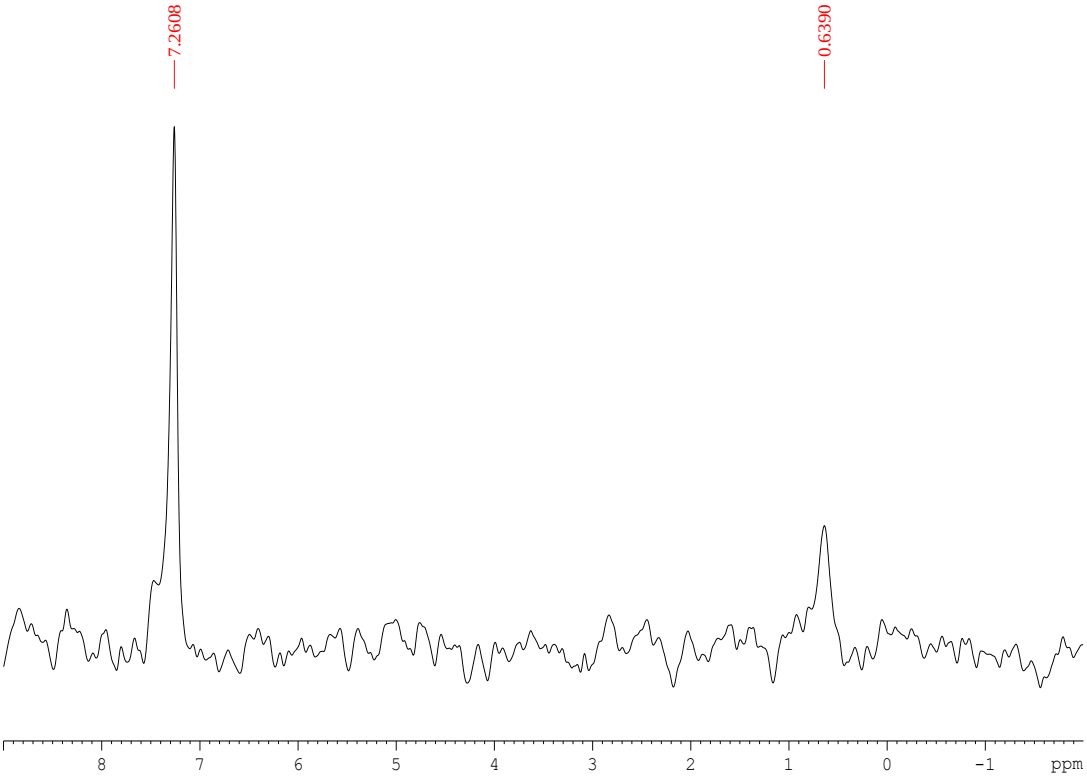

Figure S8. The ^{2}H NMR spectrum of cluster **1** in $CHCl_3$.

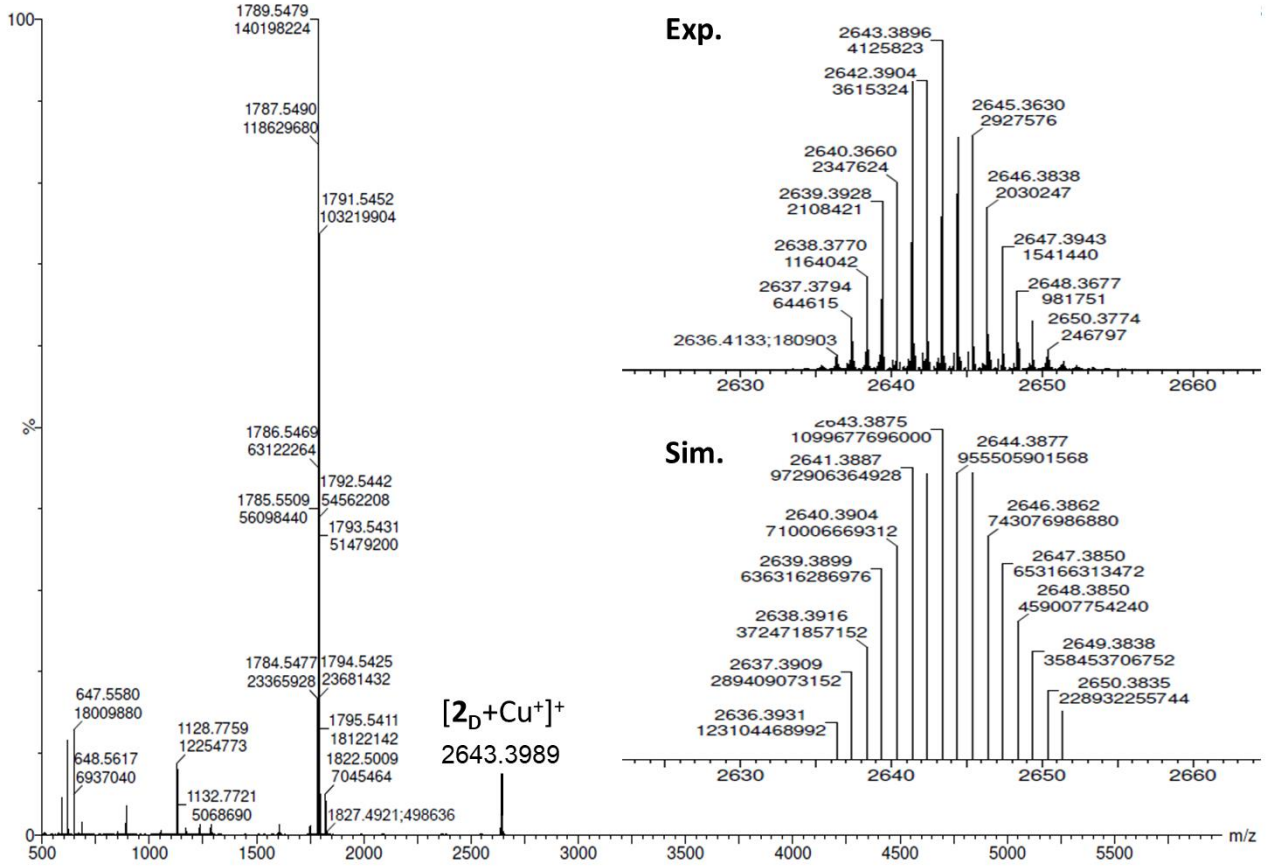

Figure S9. Positive ESI-MS spectra of the cluster [$\mathbf{2}_{D}$+Cu^{+}]$^{+}$. The inset shows the isotope pattern of the experimental one at the top and the simulation at the bottom.

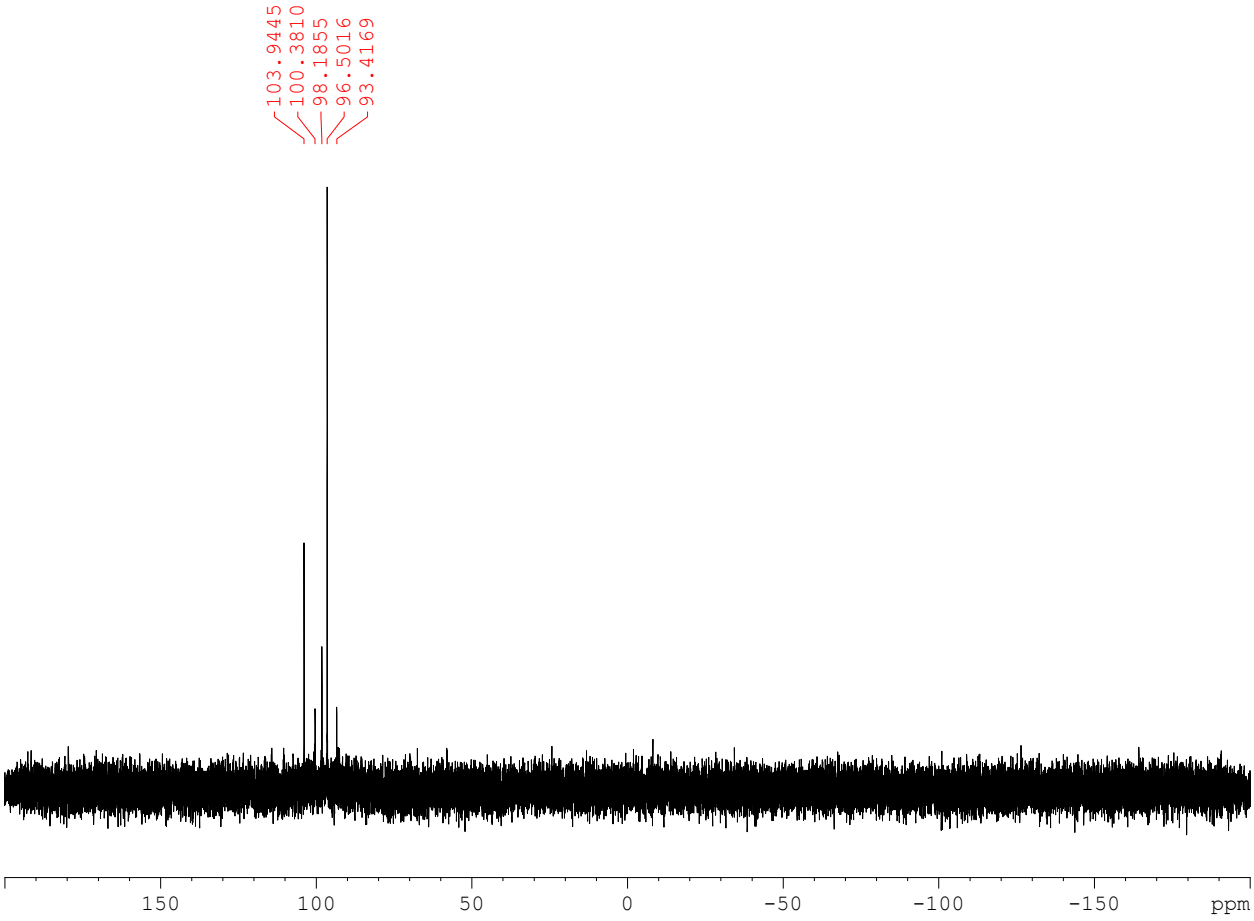

Figure S10. The $^{31}P\{^{1}H\}$ NMR spectrum of cluster **2** in d_6-acetone.

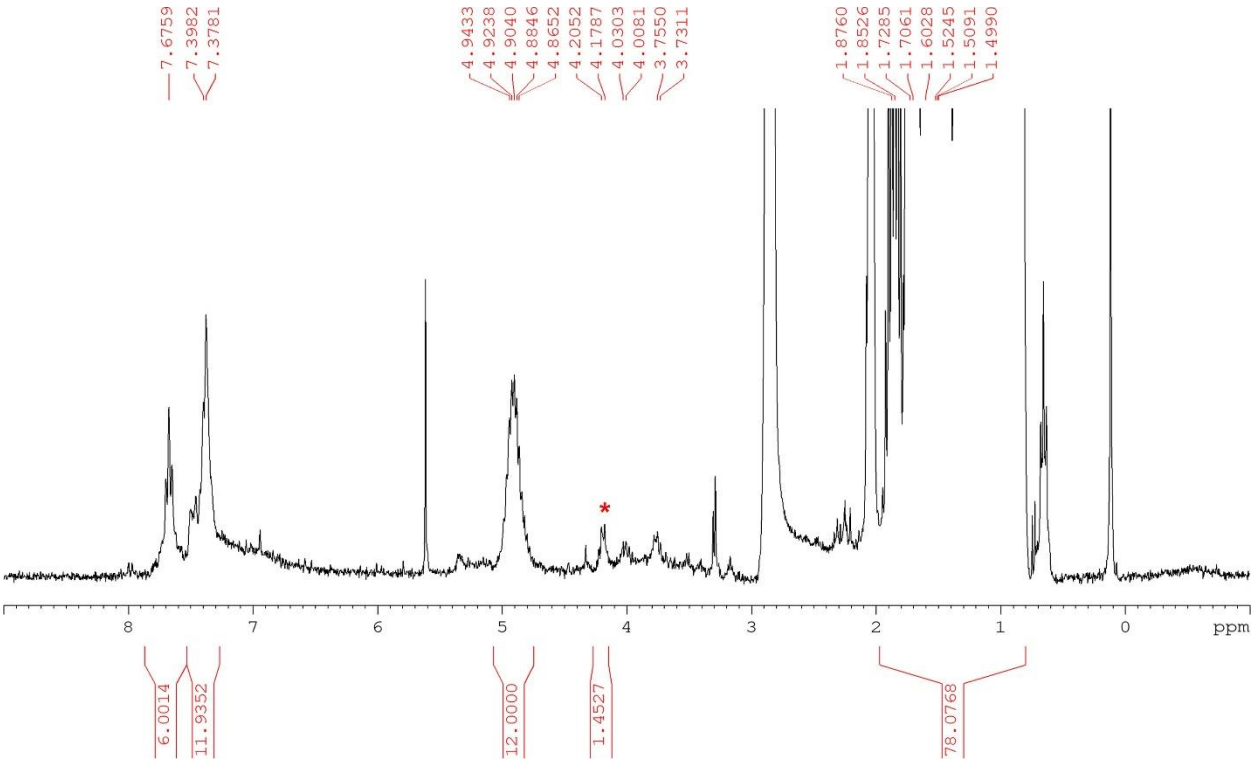

Figure S11. The ^{1}H NMR spectrum of cluster **2** in d_6-acetone.

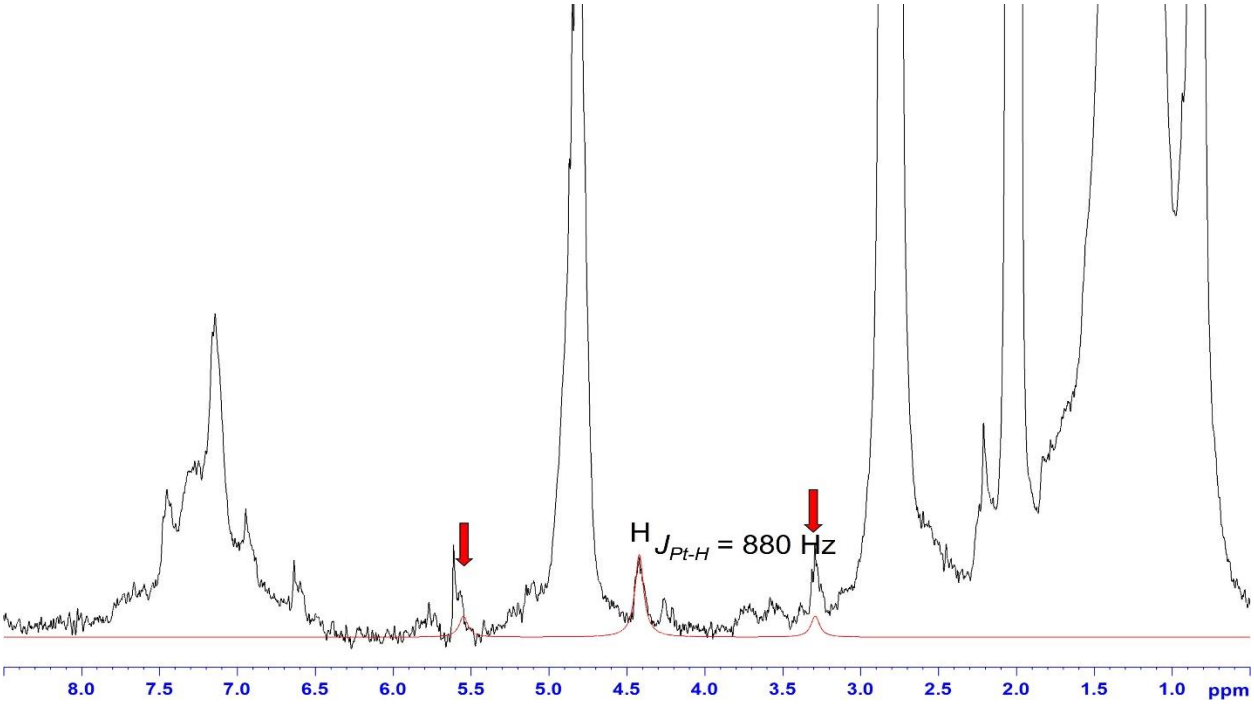

Figure S12. $^{1}H\{^{195}Pt\}$ NMR spectrum of experimental (black) and simulation (red) of cluster **2** in d_6-acetone.

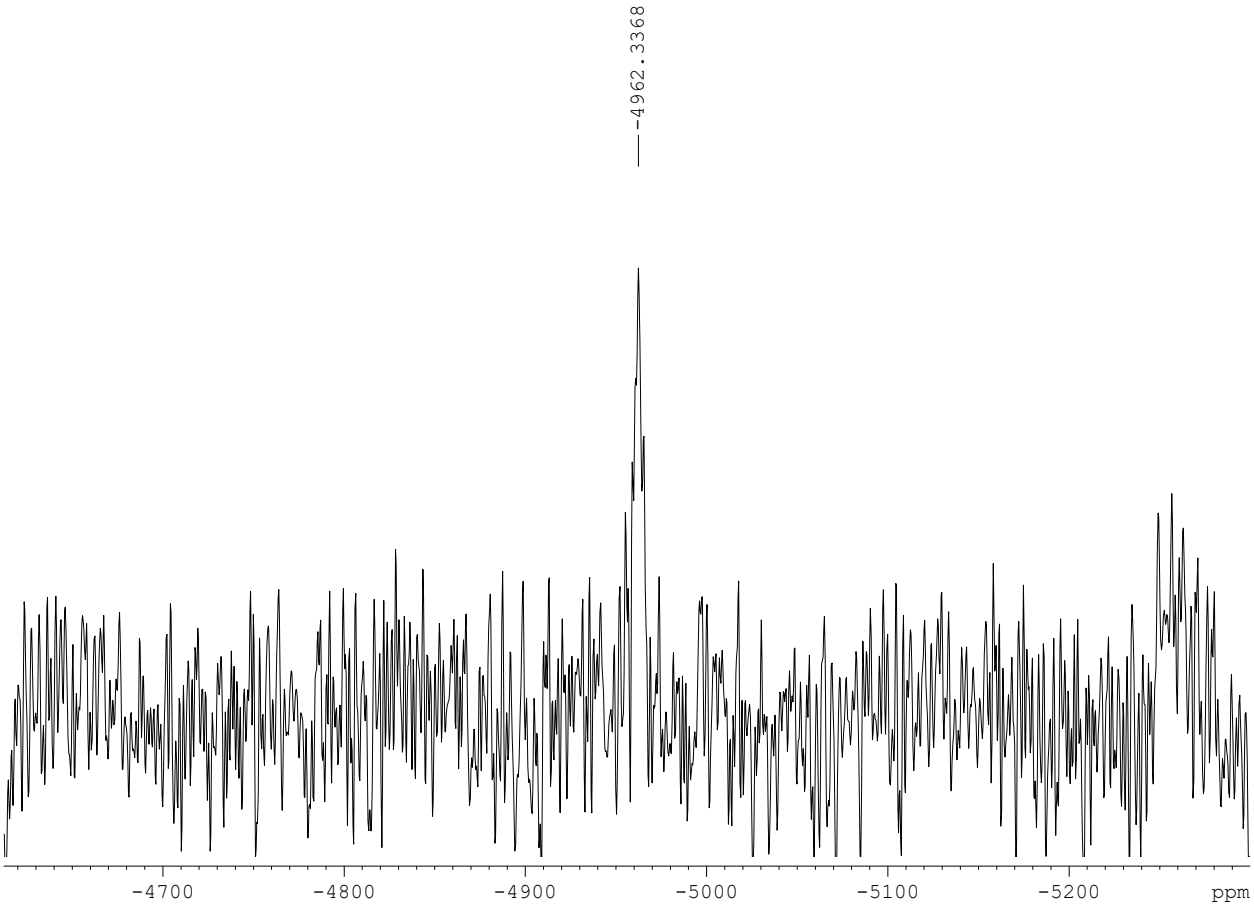

Figure S13. The $^{195}Pt\{^{1}H\}$ NMR spectrum of cluster **2** in CD_3Cl.

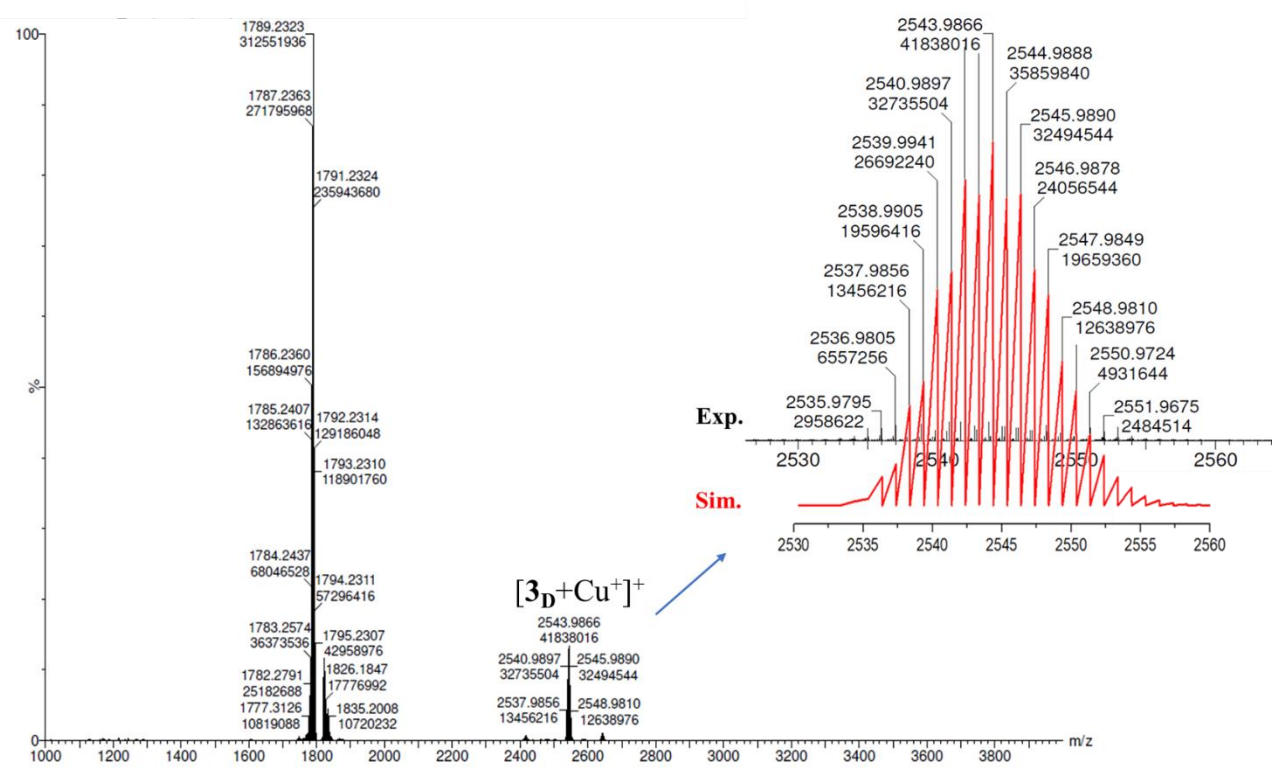

Figure S14. Positive ESI-MS spectra of the cluster $[\mathbf{3_D}+Cu^+]^+$. The inset shows the isotope pattern of the experimental one at the top and the simulation at the bottom.

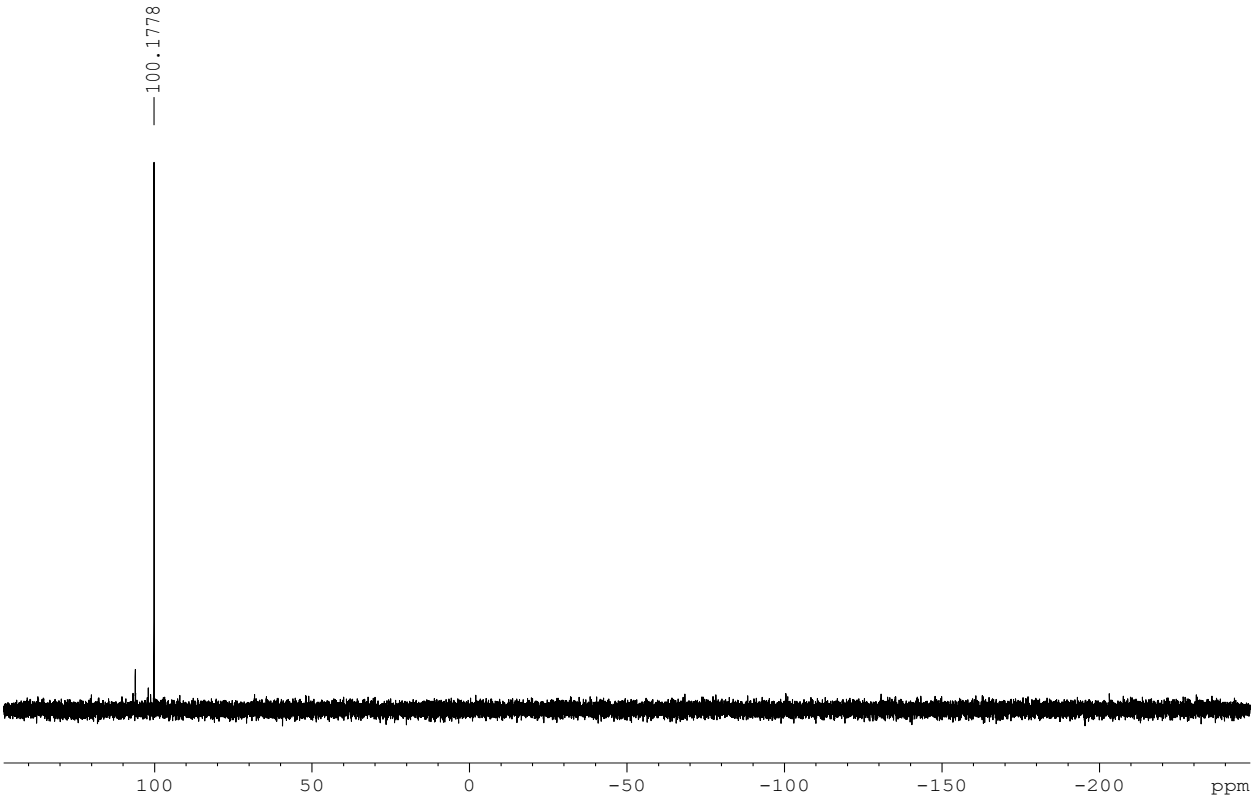

Figure S15. The $^{31}P\{^{1}H\}$ NMR spectrum of cluster **3** in $CDCl_3$.

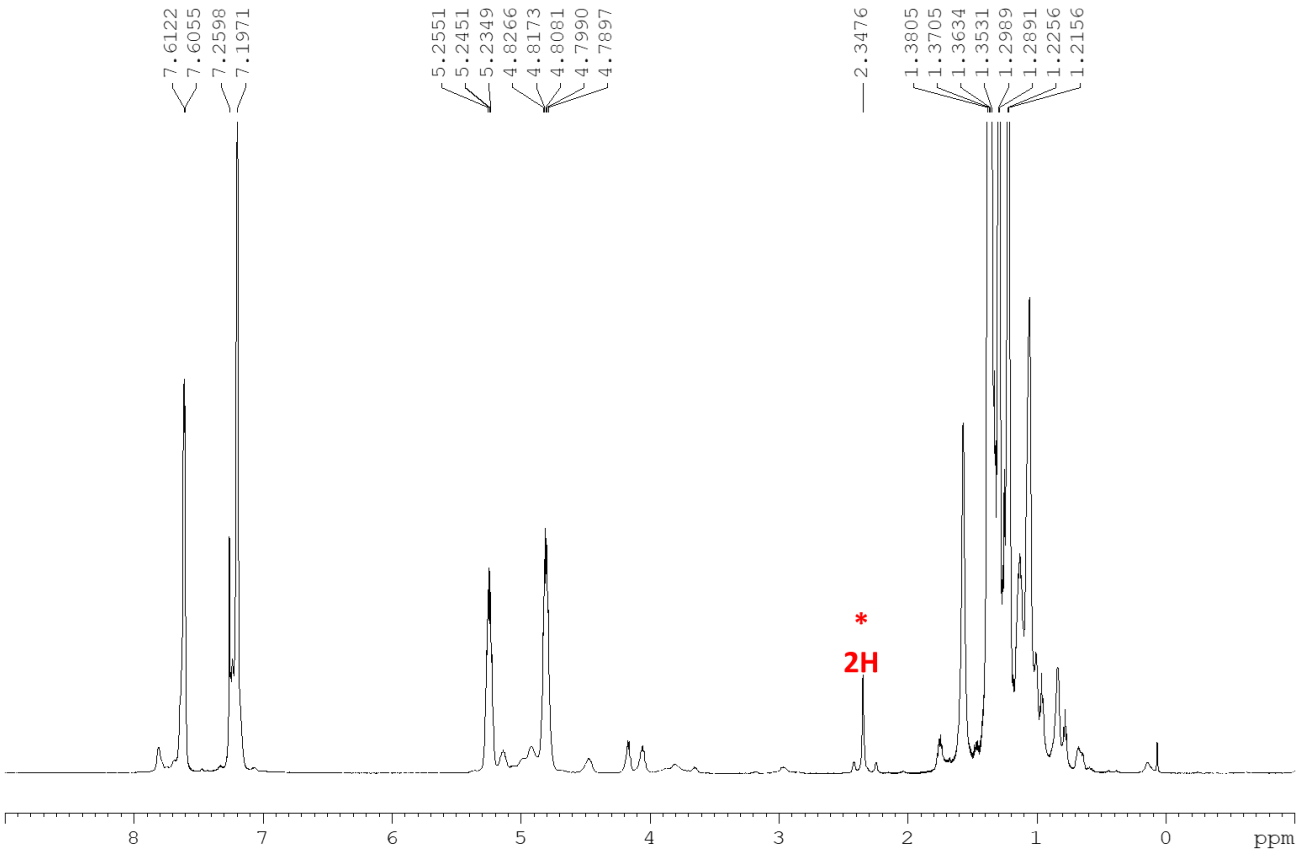

Figure S16. The ^{1}H NMR spectrum of **3** in $CDCl_3$.

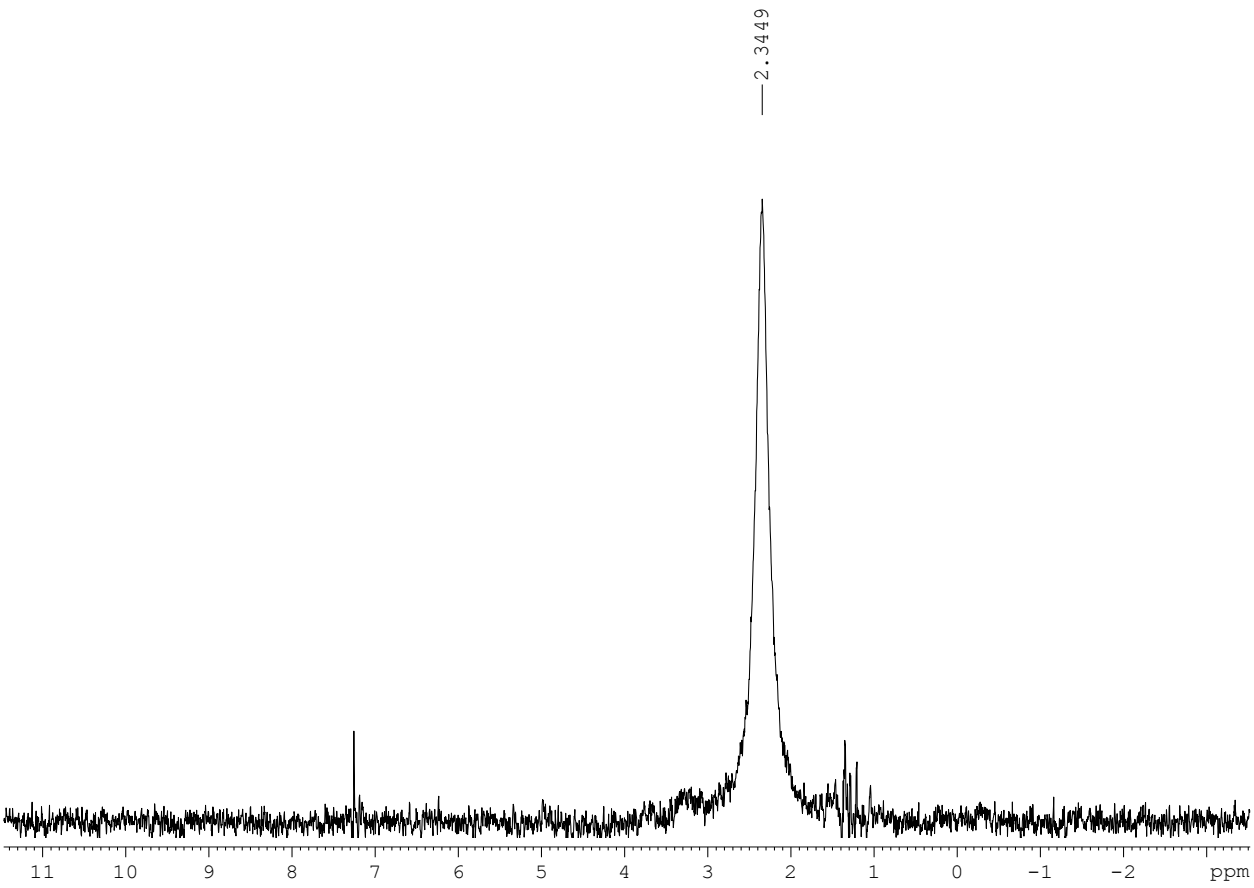

Figure S17. The $^{1}H\{^{195}Pt\}$ 1D-HMQC with decoupling spectrum of cluster **3** in $CDCl_3$.

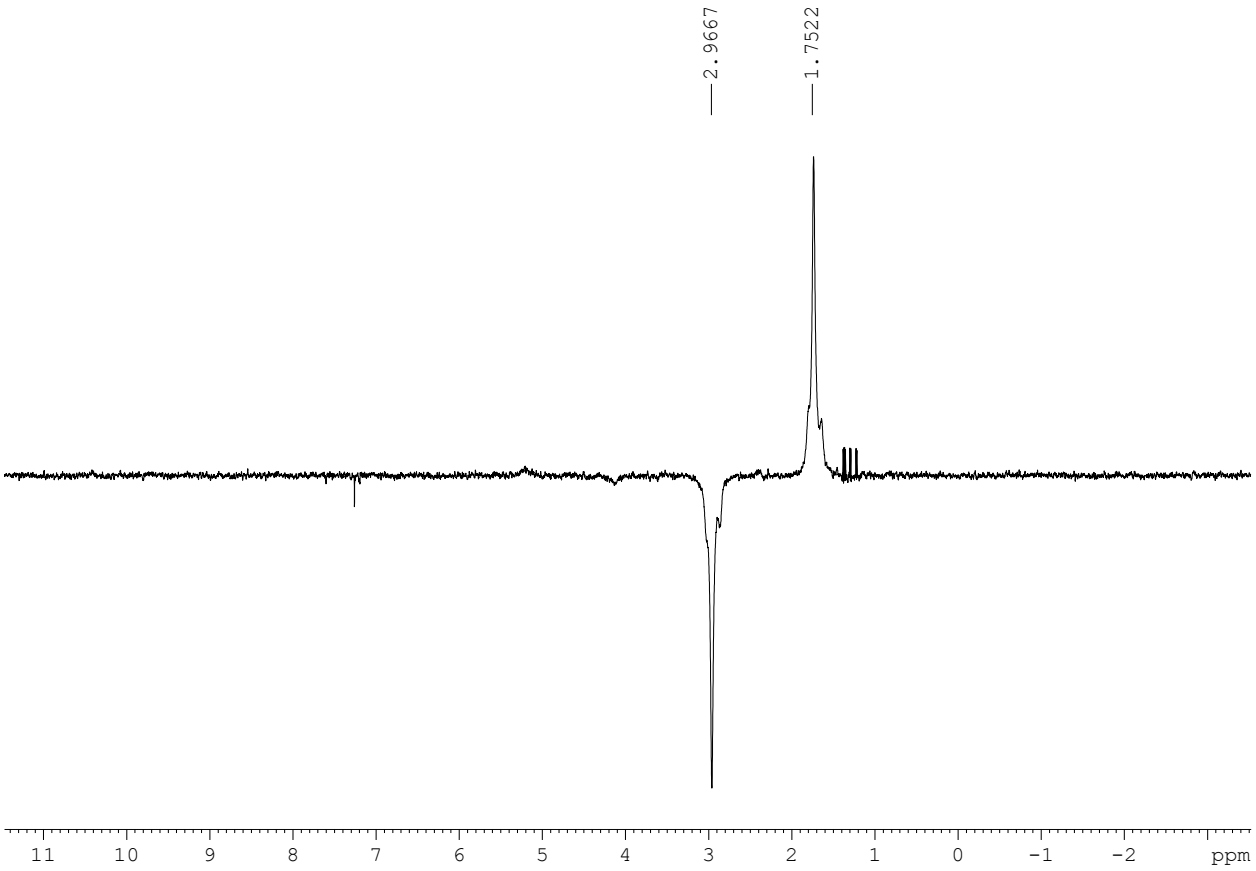

Figure S18. The $^{1}H\{^{195}Pt\}$ 1D-HMQC without decoupling spectrum of cluster **3** in $CDCl_3$.

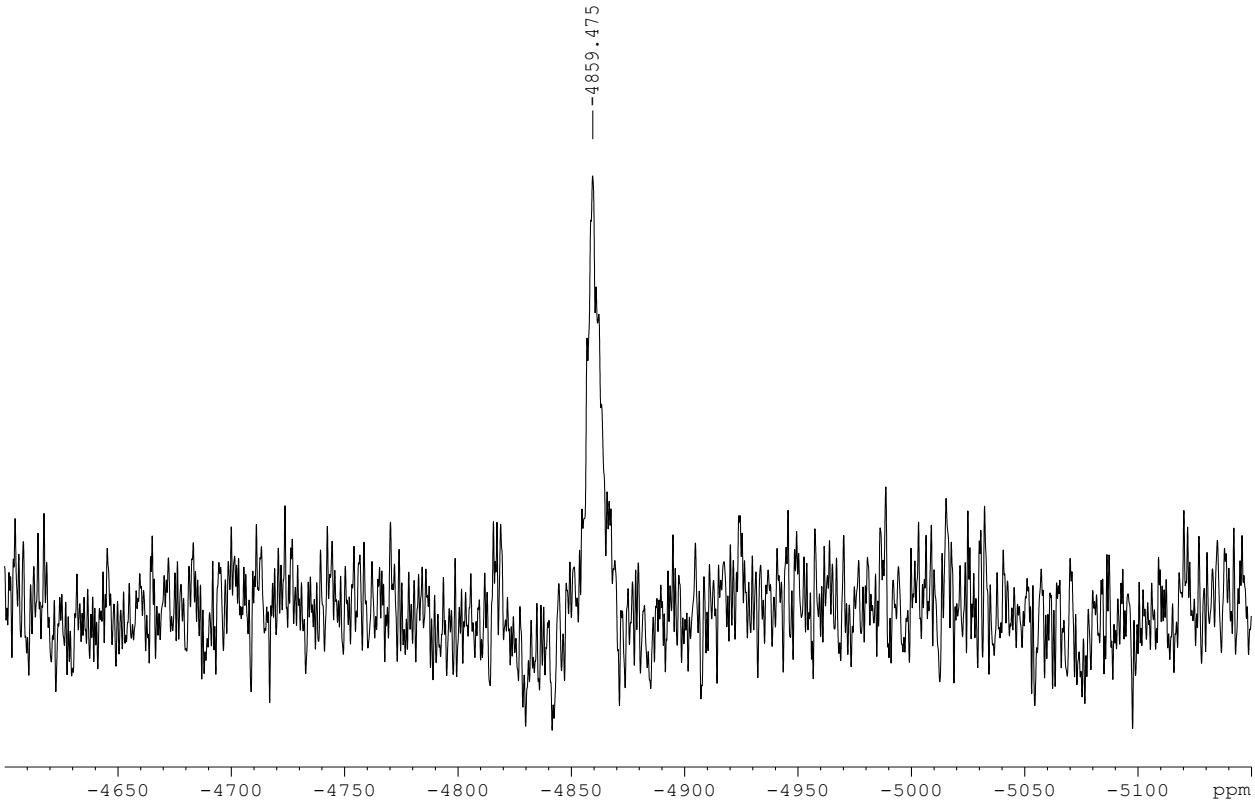

Figure S19. The ^{195}Pt NMR spectrum of cluster **3** in $CDCl_3$.

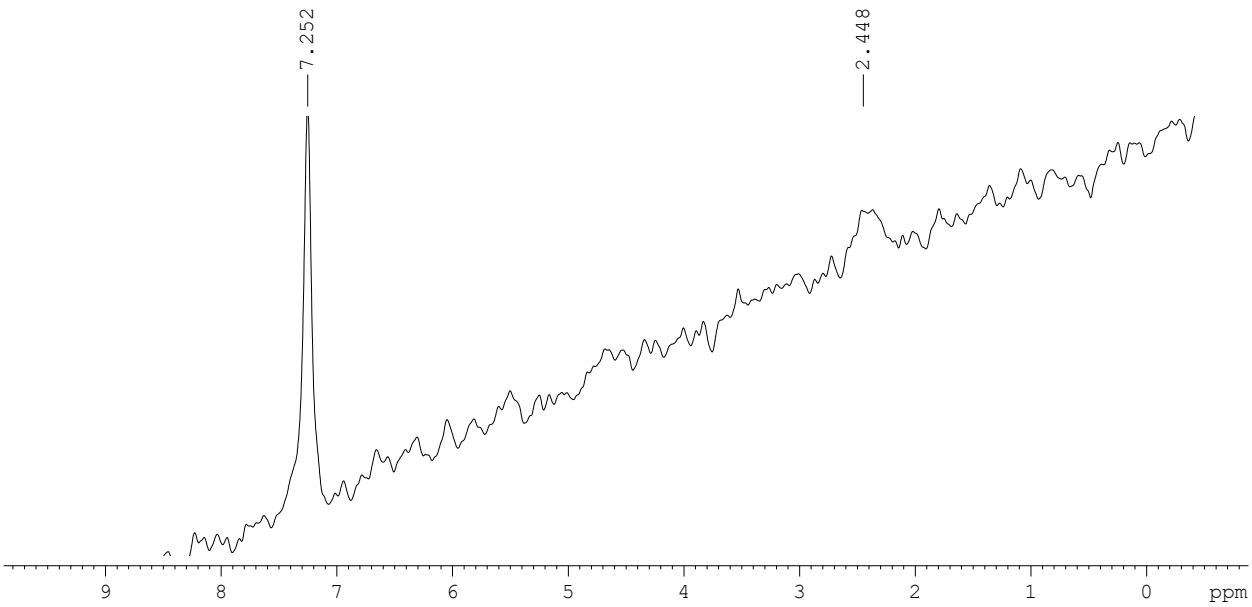

Figure S20. The ^{2}H NMR spectrum of cluster **3** in $CHCl_3$.

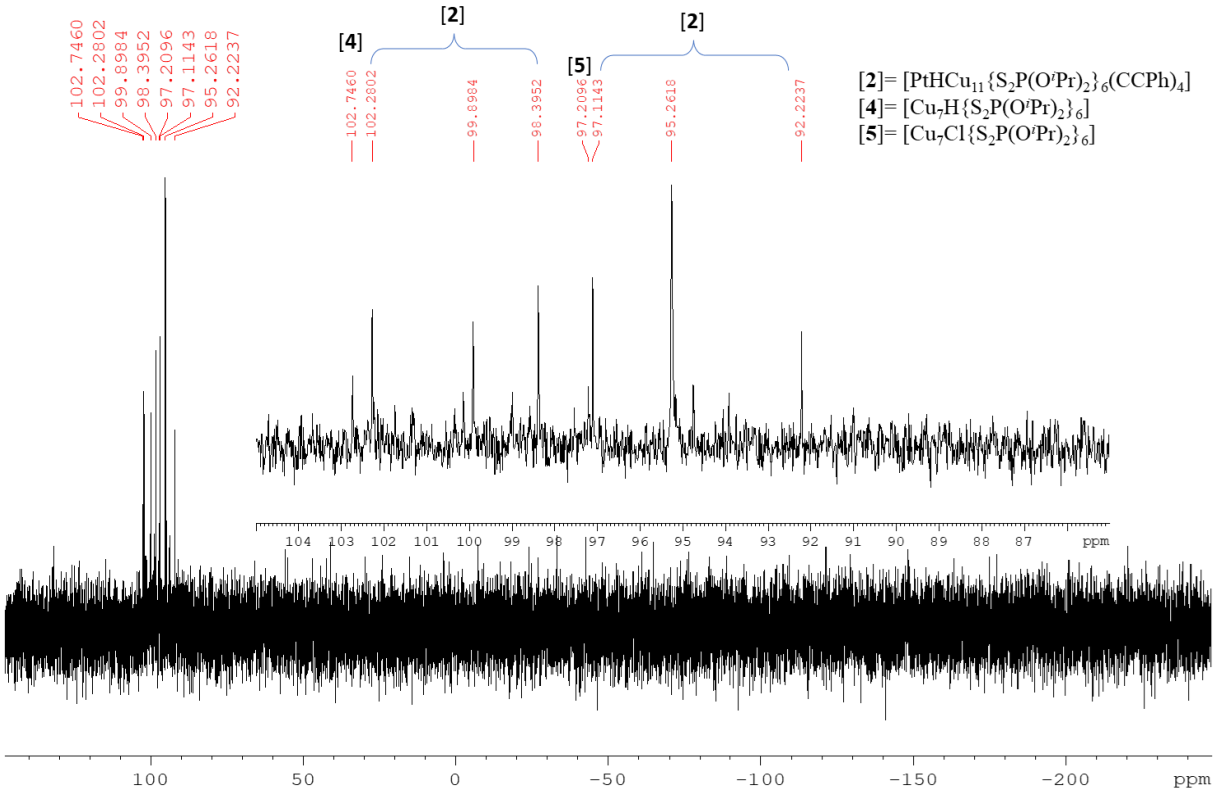

Figure S21. The $^{31}P\{^{1}H\}$ NMR spectrum of co-crystal ([**2**]$_2$ · [**4**]$_{0.85}$ · [**5**]$_{0.15}$) in $CDCl_3$.

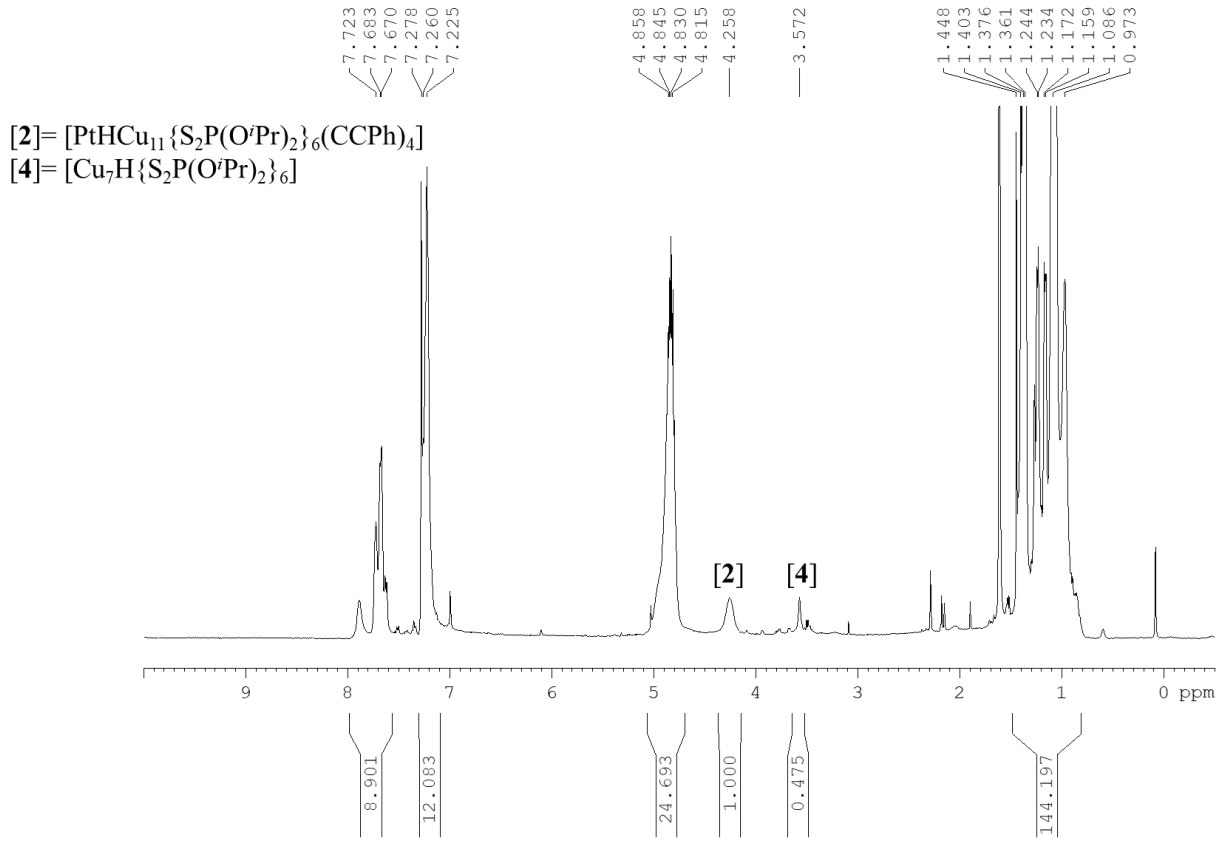

Figure S22. The ^{1}H NMR spectrum of co-crystal ([**2**]$_2$ · [**4**]$_{0.85}$ · [**5**]$_{0.15}$) in $CDCl_3$.

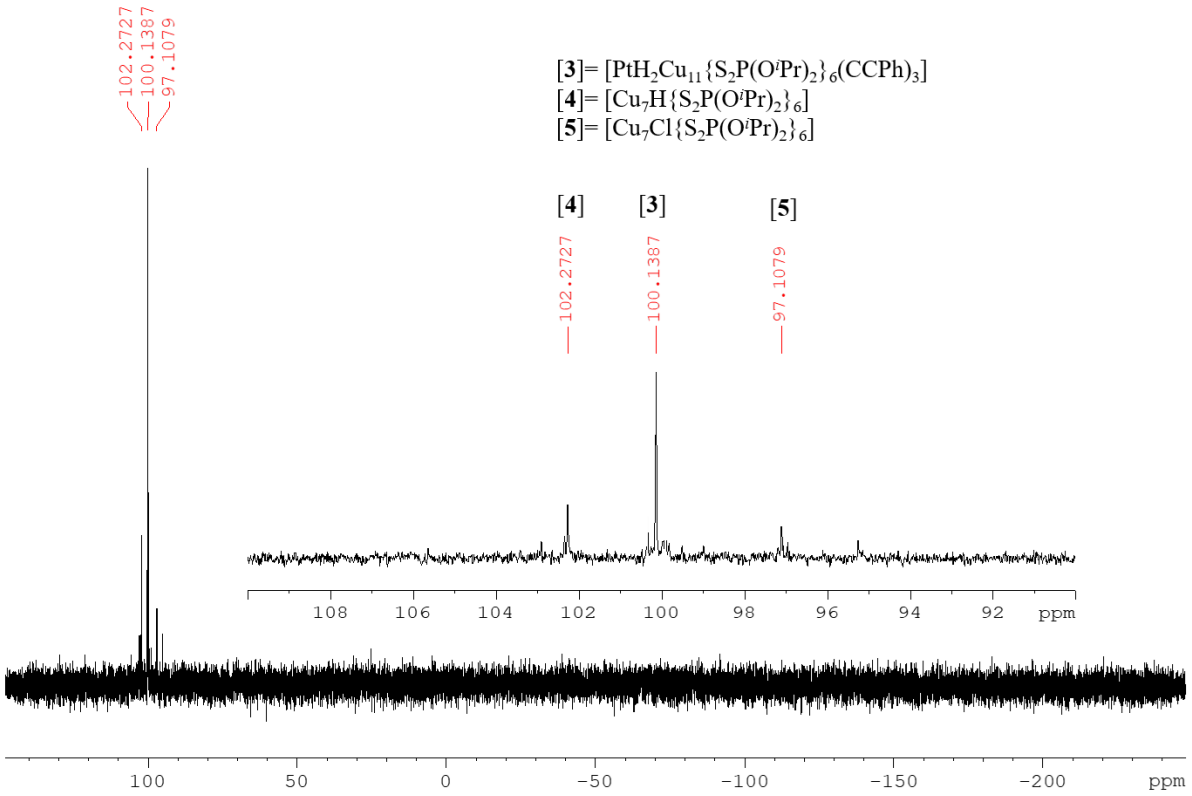

Figure S23. The $^{31}P\{^{1}H\}$ NMR spectrum of co-crystal ([**3**]$_2$ · [**4**]$_{0.75}$ · [**5**]$_{0.25}$) in $CDCl_3$.

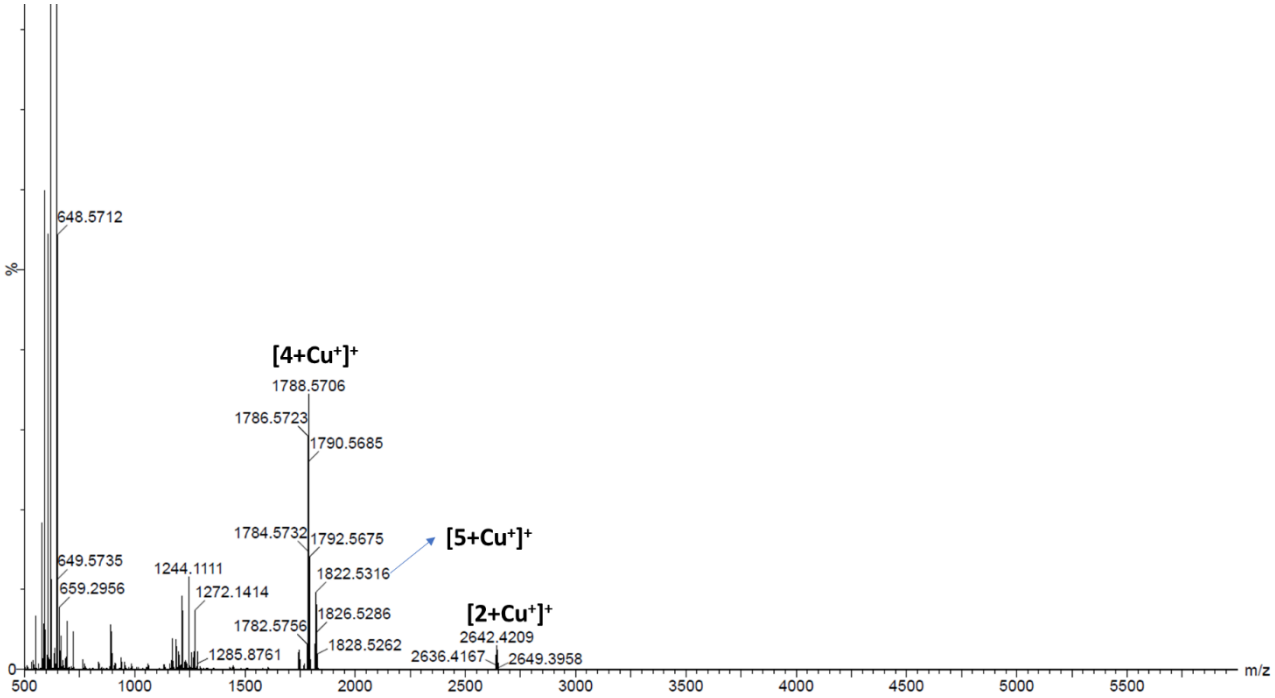

Figure S24. The positive mode of ESI-MS spectrum of co-crystal ($[\mathbf{2}]_2 \cdot [\mathbf{4}]_{0.85} \cdot [\mathbf{5}]_{0.15}$).

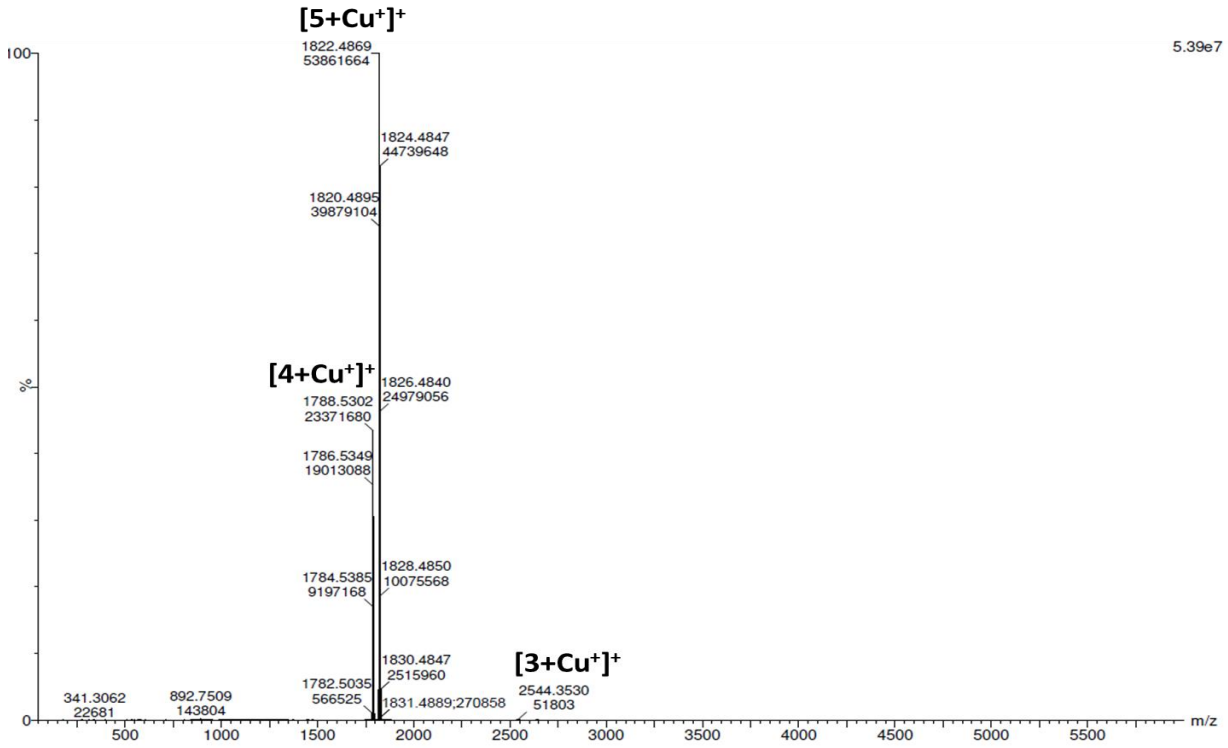

Figure S25. The positive mode of ESI-MS spectrum of co-crystal ([**3**]$_2$ · [**4**]$_{0.75}$ · [**5**]$_{0.25}$).

a)

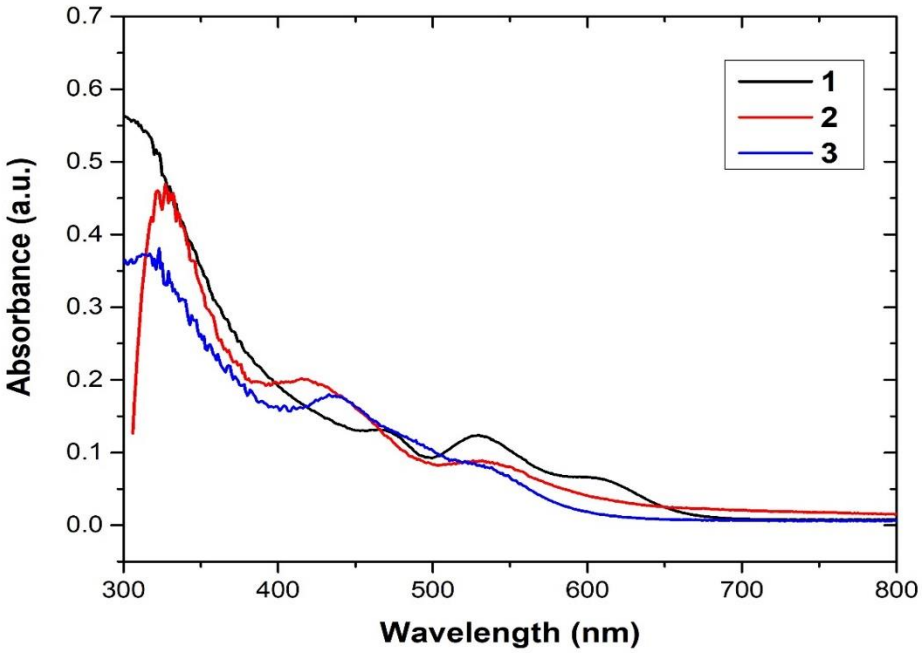

b)

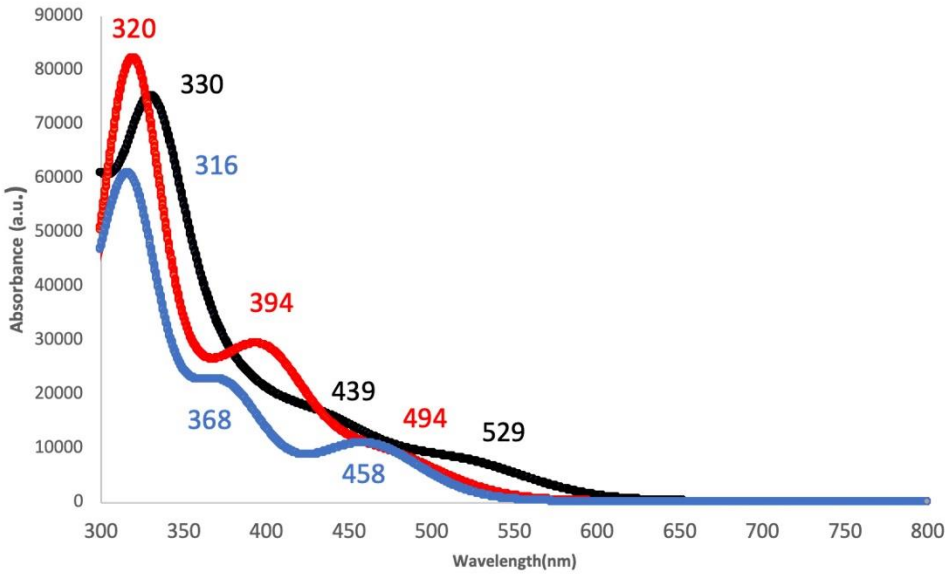

Figure S26. a) The absorption spectra **of 1, 2,** and **3** clusters in Me-THF at ambient temperature. b) The TD-DFT simulated absorption spectra of **1**(black)**, 2**(red)**,** and **3**(blue).

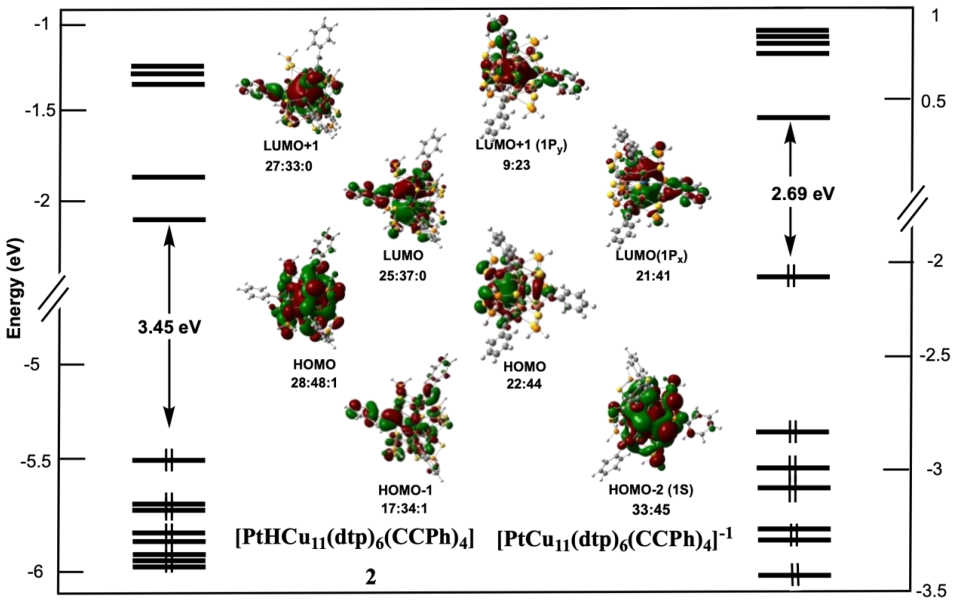

Figure S27. Kohn-Sham orbital diagrams of **2** and its deprotonated form $[PtCu_{11}(dtp)_6(C{\equiv}CPh)_4]^-$. Orbital localization (%) is given in the order Pt/Cu/H and Pt/Cu, respectively.

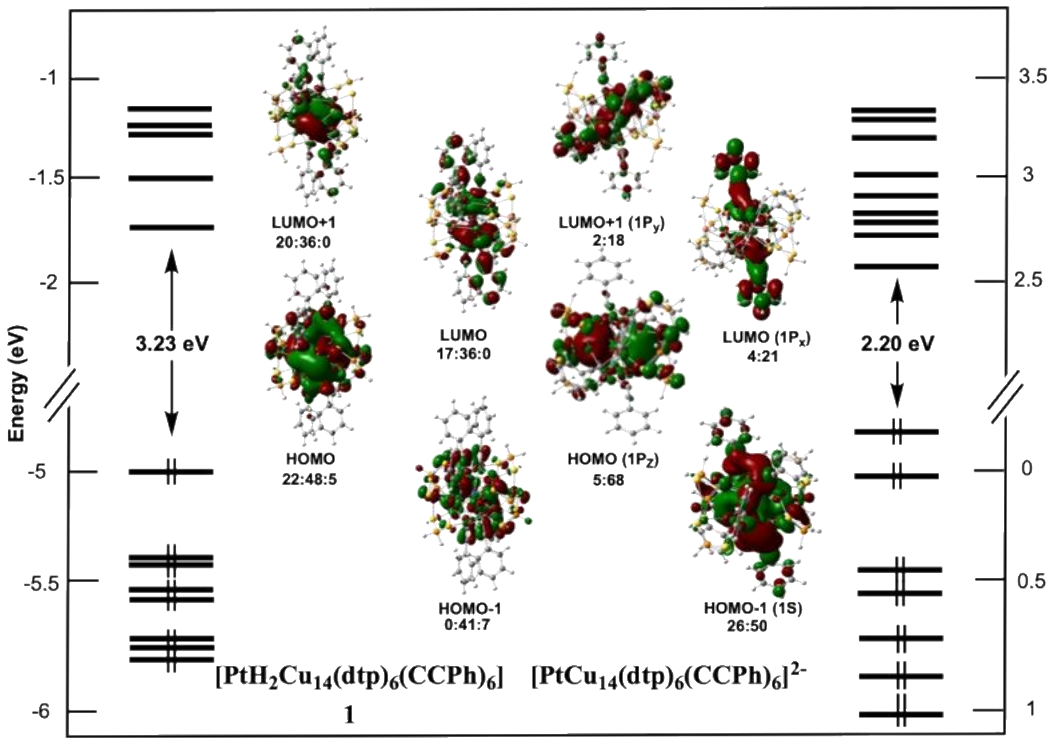

Figure S28. Kohn-Sham orbital diagrams of **1** and its deprotonated form $[PtCu_{14}(dtp)_6(CCPh)_6]^{2-}$. Orbital localization (%) is given in the order Pt/Cu/H and Pt/Cu, respectively.

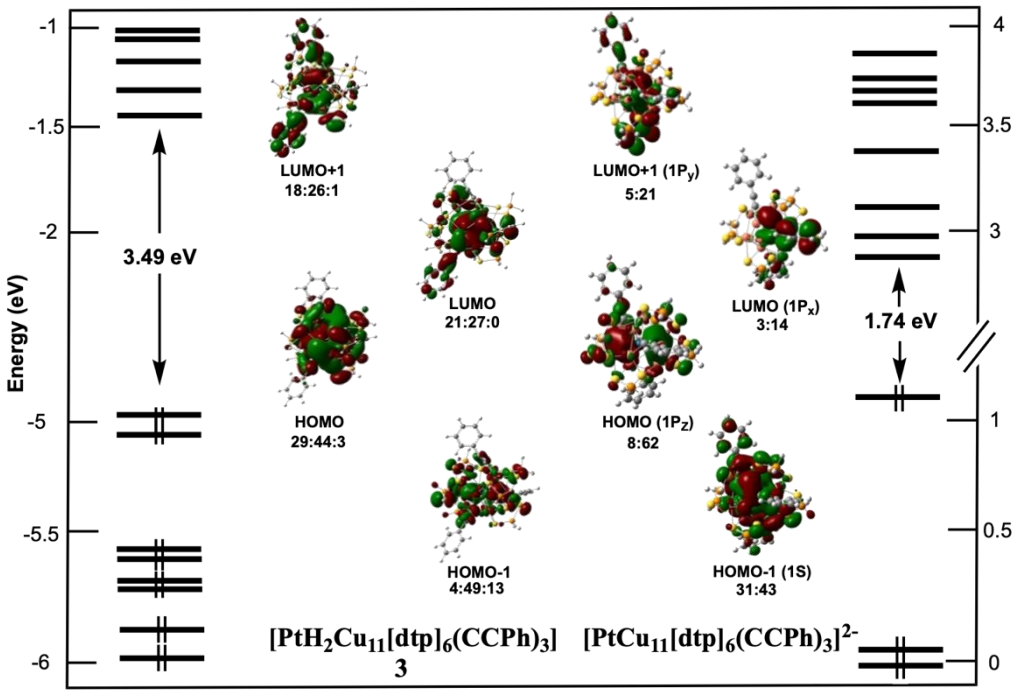

Figure S29. Kohn-Sham orbital diagrams of **3** and its deprotonated form $[PtCu_{11}(dtp)_6(CCPh)_3]^{2-}$. Orbital localization (%) is given in the order Pt/Cu/H and Pt/Cu, respectively.

Table S1. Selected X-ray crystallographic data of **1**, $[\mathbf{2}]_2{\cdot}[\mathbf{4}]_{0.85}\cdot[\mathbf{5}]_{0.15}$, $[\mathbf{3}]_2{\cdot}[\mathbf{4}]_{0.75}\cdot[\mathbf{5}]_{0.25}$, and neutron data of $\mathbf{1_N}$.

	$\mathbf{1}\cdot(C_6H_6)$	$\mathbf{1_N}\cdot(C_6H_6)$	$[\mathbf{2}]_2{\cdot}[\mathbf{4}]_{0.85}\cdot[\mathbf{5}]_{0.15}$	$[\mathbf{3}]_2{\cdot}[\mathbf{4}]_{0.75}\cdot[\mathbf{5}]_{0.25}$
CDCC no.	2296486	2296487	2296488	2296489
Empirical formula	$C_{90}H_{122}Cu_{14}O_{12}P_6PtS_{12}$	$C_{90}H_{122}Cu_{14}O_{12}P_6PtS_{12}$	$C_{172}H_{294.85}Cl_{0.15}Cu_{29}O_{36}P_{18}Pt_2S_{36}$	$C_{156}H_{286.75}Cl_{0.25}Cu_{29}O_{36}P_{18}Pt_2S_{36}$
Formula weight	3051.20	3051.06	6888.69	6736.09
Temperature, K	100(2)	100(2)	100(2)	100(2)
Wavelength, Å	0.71073	0.700	0.71073	0.71073
Crystal system	Triclinic	Triclinic	Triclinic	Triclinic
Space group	*P*(-)1	*P*(-)1	*P*(-)1	*P*(-)1
a, Å	15.2774(9)	15.3150(11)	15.402(2)	14.5301(9)
b, Å	15.4879(9)	15.5321(11)	20.602(3)	20.1634(13)
c, Å	25.1123(15)	25.0855(17)	23.689(3)	23.4158(14)
α, deg.	87.031(1)	87.112(7)	108.430(3)	106.050(1)
β, deg.	85.789(1)	86.002(6)	106.585(3)	102.114(1)
γ, deg.	70.357(1)	70.685(7)	98.079(3)	98.411(2)
Volume, $Å^3$	5578.7(6)	5615.3(7)	6610.4(17)	6291.8(7)
Z	2	2	1	1
Calculated density, Mg m^{-3}	1.816	1.805	1.730	1.766
Absorption coefficient, mm^{-1}	4.218	0.11544 + 0.08547λ	3.779	3.968
Crystal size, mm^3	0.32 x 0.27 x 0.20	2.05 x 1.95 x 0.69	0.23 x 0.16 x 0.03	0.120 x 0.100 x 0.050
θ_{max}, deg.	26.00		25.00	25.00
Reflections collected / unique	40166 / 21540 (R_{int} = 0.0275)	39436 / 12960 (R_{int} = 0.0741)	53714 / 23020 (R_{int}= 0.0557)	36963 / 21907 (R_{int}= 0.0375)
Completeness, %	98.7		98.9	98.8
restraints / parameters	558 / 1251	0 / 1970	850 / 1498	656 / 1328
GOF	1.032	1.044	1.062	1.032
[a] *R*1, [b] *wR*2 [I > 2σ(I)]	*R*1 = 0.0292, *wR*2 = 0.0750	*R*1 = 0.0515, *wR*2 = 0.0985	*R*1 = 0.0767, *wR*2 = 0.1857	*R*1 = 0.0614, *wR*2 = 0.1475
[a] *R*1, [b] *wR*2 (all data)	*R*1 = 0.0348, *wR*2 = 0.0795	*R*1 = 0.0559, *wR*2 = 0.0972	*R*1 = 0.1113, *wR*2 = 0.2072	*R*1 = 0.1012, *wR*2 = 0.1755
Largest diff. peak / hole, e $Å^{-3}$ (neutron, fm)	1.538, -2.150	0.994, -0.698	3.248, -2.100	2.008, -1.474

[a] $R1 = \Sigma\,||F_o| - |Fc||/\Sigma|F_o|$. [b] $wR2 = \{\Sigma[w(F_o^2 - F_c^2)^2]/\Sigma[w(F_o^2)^2]\}^{1/2}$.

Table S2. Comparison of HER activities measured on bimetallic nanocluster catalysts.

Nanocluster	Onset Potential (V vs. RHE)	TOF (s^{-1})	Electrolyte	References
$PtHCu_{11}$	~0	526@0.1V	0.5 M H_2SO_4	This work
$[PdHCu_{11}\{S_2P(O^iPr)2\}_6(CCPh)_3]$	-0.05	250@0.1V	0.5 M H_2SO_4	*Angew. Chem. Int. Ed.* **2023**, *62*, e202301272
Pt_1Ag_{28}-BTT-Mn	-0.10	-	0.5 M H_2SO_4	*Nanoscale.* **2023**, *15*, 14941-14948
$Ag_{20}Rh_2(C{\equiv}C\text{-}^tBu)_{16}(CF_3CO_2)_6(H_2O)_2$	-0.1 (@10 mA cm^{-2})	-	0.5 M H_2SO_4	*Chem Asian J.* **2023**, e202300685
$Au_9Ag_9(CCAr^F)_{18}$	–0.10	-	0.5 M H_2SO_4	*Eur. J. Inorg. Chem.* **2022**, e202200176.
$Au_{24}Ag_{20}(^tBuC{\equiv}C)_{24}Cl_2$	–0.25	-	0.5 M H_2SO_4	*Dalton Trans*. **2022**, *51*, 7845–7850.
$Au_{22}Ag_{22}(^tBuC{\equiv}C)_{16}Br_{3.3}Cl_{2.7}$	–0.15	-		
$Au_{36}Ag_2(S\text{-}Adm)_{18}$	–0.10	-	0.5 M H_2SO_4	*J. Am. Chem. Soc*. **2021**, *143*, 11102-11108.
$NiAg_{24}(SPhMe_2)_{18}$	–0.05	108.5@0.60V	1.0 M KOH	*Bull. Korean Chem. Soc*. **2021**, *42*, 1672–1677
$Au_2Pd_6S_4(PPh_3)_4(SC_6H_4F_2)_6$	–0.15	1.15@0.4V	0.5 M H_2SO_4	*Inorg. Chem. Front*. **2018**, *5*, 2948-2954.
$PdAu_{24}(SC_6H_{13})_{18}$	–0.07	13.0@0.60V	[a]1.0 M B-R buffer (pH 3)	*ACS Appl. Mater. Interfaces* **2018**, *10*, 44645−44653.
$Pt_2Au_{36}(SC_6H_{13})_{24}$	–0.20	28.2@0.60V		
$Pd_2Au_{36}(SC_6H_{13})_{24}$	–0.07	13.1@0.60V		
$PtAu_{24}(SC_6H_{13})_{18}$	–0.07	34.0@0.60V	[a]1.0 M B-R buffer (pH 3)	*Nat. Commun*. **2017**, 14723.

[a] B-R buffer: Britton-Robinson buffer

Table S3. Comparison of HER activities measured on $PtHCu_{11}$ with single-atom catalysts in acidic media (0.5 M H_2SO_4).

Catalyst	Tafel slope (mV dec^{-1})	η at 10 mA cm^{-2} (mV)	TOF (s^{-1})	Reference
$PtHCu_{11}$	39	30	526@0.1V	This work
ZnNiCoIrMn	31	31	6.4@0.03V	*Adv. Mater*. **2023**, *35*, 2300091.
PBN-300-Ir	17	25	171@0.1V	*Adv. Sci*. **2022**, *9*, 2105392.
IrMo/CNT	22	17	15@0.05V	*Nat. Commun*. **2022**, *13*, 5497.
Pt SA/C-Air	27	8	13@0.1V	*Appl. Catal. B: Environ*. **2021**, *285*, 119861.
Pt-SAs/WS_2	28	32	273@0.2V	*Nat. Commun*. **2021**, *12*, 3021.
Pt_1/OLC	36	38	41@0.1V	*Nat. Energy*. **2019**, *4*, 512–518.
Pt SA/WO_{3-x}	45	38	35@0.1V	*Angew. Chem. Int. Ed*. **2019**, *58*, 16038–16042.
Pt/hCNC	24	15	7.67@0.02V	*Nat. Commun*. **2019**, *10*, 1657.
Pt_1/NPC	28	25	100@0.1V	*ACS Catal*. **2018**, *8*, 8450–8458.

Table S4. Cartesian coordinates of the DFT-optimezed structures of **1**, **2**, and **3**.

$[PtH_2Cu_{14}\{S_2P(O^iPr)_2\}_6(CCPh)_6]$ (**1**)

Pt	0.000000	0.000000	0.000000
Cu	-3.605225	-0.050100	1.881289
Cu	-2.636065	0.637413	-0.697566
Cu	-1.640401	-1.965556	1.195659
Cu	-1.146643	1.130254	2.249066
Cu	0.805988	-0.713662	2.546802
Cu	-1.421540	-1.830739	-1.462835
Cu	0.688648	-2.650439	0.156147
Cu	3.605225	0.050100	-1.881289
Cu	2.636065	-0.637413	0.697566
Cu	1.640401	1.965556	-1.195659
Cu	1.146643	-1.130254	-2.249066
Cu	-0.805988	0.713662	-2.546802
Cu	1.421540	1.830739	1.462835
Cu	-0.688648	2.650439	-0.156147
S	-2.808405	0.554465	3.943951
S	-0.828342	-2.290943	3.444404
S	-1.914558	3.390259	1.808802
S	-4.569037	1.494832	0.508211
S	-4.040053	-2.270145	1.570564
S	-3.763198	-1.242092	-1.767713
S	2.808405	-0.554465	-3.943951
S	0.828342	2.290943	-3.444404
S	1.914558	-3.390259	-1.808802
S	4.569037	-1.494832	-0.508211
S	4.040053	2.270145	-1.570564
S	3.763198	1.242092	1.767713
C	-0.703922	-1.091597	-3.308453
C	-0.901862	-2.090775	-4.004409

C	-1.132004	-3.213097	-4.844982
C	-0.064528	-4.009700	-5.276319
H	0.940622	-3.758702	-4.959453
C	-0.298075	-5.105976	-6.088030
H	0.535286	-5.717689	-6.414403
C	-1.590737	-5.422676	-6.484555
H	-1.768518	-6.280184	-7.123551
C	-2.654939	-4.636740	-6.061857
H	-3.665743	-4.880442	-6.368752
C	-2.433044	-3.541090	-5.246225
H	-3.258356	-2.927137	-4.905879
C	-1.176305	-3.427773	-0.177292
C	-1.526465	-4.562937	-0.504417
C	-1.922689	-5.881856	-0.844024
C	-1.972833	-6.294733	-2.182211
H	-1.703833	-5.594832	-2.964351
C	-2.361149	-7.584519	-2.498728
H	-2.395913	-7.889660	-3.538427
C	-2.701158	-8.482808	-1.496049
H	-3.003680	-9.492428	-1.749394
C	-2.652404	-8.083156	-0.166885
H	-2.917394	-8.780101	0.620197
C	-2.268993	-6.795111	0.161690
H	-2.231354	-6.476839	1.196726
C	1.964025	-2.200706	1.818239
C	2.086046	-3.429214	1.930147
C	2.353087	-4.798529	2.204210
C	1.698609	-5.820939	1.506131
H	0.973129	-5.558623	0.744857
C	1.977250	-7.147063	1.787984
H	1.462033	-7.927601	1.239650

C	2.905203	-7.477161	2.766122
H	3.119294	-8.517015	2.984895
C	3.558206	-6.469543	3.464796
H	4.282838	-6.721473	4.230857
C	3.289916	-5.141162	3.189591
H	3.795909	-4.351607	3.731955
P	-2.039808	-1.192000	4.601562
P	-3.803125	3.248540	1.150660
P	-4.575537	-2.421253	-0.368441
C	0.703922	1.091597	3.308453
C	0.901862	2.090775	4.004409
C	1.132004	3.213097	4.844982
C	0.064528	4.009700	5.276319
H	-0.940622	3.758702	4.959453
C	0.298075	5.105976	6.088030
H	-0.535286	5.717689	6.414403
C	1.590737	5.422676	6.484555
H	1.768518	6.280184	7.123551
C	2.654939	4.636740	6.061857
H	3.665743	4.880442	6.368752
C	2.433044	3.541090	5.246225
H	3.258356	2.927137	4.905879
C	1.176305	3.427773	0.177292
C	1.526465	4.562937	0.504417
C	1.922689	5.881856	0.844024
C	1.972833	6.294733	2.182211
H	1.703833	5.594832	2.964351
C	2.361149	7.584519	2.498728
H	2.395913	7.889660	3.538427
C	2.701158	8.482808	1.496049
H	3.003680	9.492428	1.749394

C	2.652404	8.083156	0.166885
H	2.917394	8.780101	-0.620197
C	2.268993	6.795111	-0.161690
H	2.231354	6.476839	-1.196726
C	-1.964025	2.200706	-1.818239
C	-2.086046	3.429214	-1.930147
C	-2.353087	4.798529	-2.204210
C	-1.698609	5.820939	-1.506131
H	-0.973129	5.558623	-0.744857
C	-1.977250	7.147063	-1.787984
H	-1.462033	7.927601	-1.239650
C	-2.905203	7.477161	-2.766122
H	-3.119294	8.517015	-2.984895
C	-3.558206	6.469543	-3.464796
H	-4.282838	6.721473	-4.230857
C	-3.289916	5.141162	-3.189591
H	-3.795909	4.351607	-3.731955
P	2.039808	1.192000	-4.601562
P	3.803125	-3.248540	-1.150660
P	4.575537	2.421253	0.368441
H	4.379009	3.765988	0.737903
H	5.978930	2.307180	0.438470
H	-3.990376	4.180992	0.112391
H	-4.659930	3.756000	2.148365
H	-5.978930	-2.307180	-0.438470
H	-4.379009	-3.765988	-0.737903
H	-3.104100	-2.000807	5.051141
H	-1.368335	-0.917065	5.808957
H	3.990376	-4.180992	-0.112391
H	4.659930	-3.756000	-2.148365
H	1.368335	0.917065	-5.808957

H	3.104100	2.000807	-5.051141
H	-1.531490	-0.047118	0.791590
H	1.531490	0.047118	-0.791590

[$PtHCu_{11}\{S_2P(O^iPr)_2\}_6(CCPh)_4$] (**2**)

Pt	-0.001731	-0.068697	0.349297
C	0.042430	0.155804	2.336099
Cu	-0.193336	-1.910581	2.320054
Cu	2.738364	-0.703656	0.253536
Cu	1.564173	2.261891	0.032510
Cu	-2.765687	0.285020	-0.049183
Cu	-1.859797	-2.196416	0.102152
Cu	1.301768	-1.329636	-1.947774
Cu	-1.516691	1.525809	2.088572
Cu	1.076289	-2.833513	0.136578
Cu	-1.080066	2.671744	-0.338912
H	-0.014528	-0.202528	-1.322490
S	-1.557133	3.776820	1.717090
S	-3.678240	0.587901	2.147418
C	0.042781	0.480132	3.535614
S	3.567638	-0.899982	2.435227
S	1.337743	-3.606172	2.382738
S	-2.395789	-2.704020	2.384741
C	0.492169	3.247982	-1.466341
S	3.640143	1.316743	-0.502514
S	1.898473	3.298275	2.099517
Cu	0.207450	1.398033	-2.166331
S	-3.306008	2.359636	-1.031222
C	-3.222721	-1.402772	-1.202470
Cu	-1.514198	-0.869464	-2.097383
S	-0.742830	-4.197752	-0.462382

C	2.697963	-2.387086	-0.978132
S	1.979301	0.409888	-3.478766
S	-1.601181	0.912040	-3.724072
C	1.009908	4.326299	-1.762146
S	-0.262786	-2.424877	-3.446727
P	0.332918	4.494119	1.994054
P	-3.291582	-1.090680	3.191787
P	3.209166	-2.834942	2.608021
P	3.548384	1.199578	-2.511769
P	-3.234697	1.778283	-2.960542
P	-0.803425	-4.086000	-2.472564
C	0.255157	0.834565	4.897388
C	1.474205	0.530121	5.516404
C	-0.734441	1.495218	5.634752
C	1.685020	0.871478	6.839908
H	2.245488	0.035495	4.937786
C	0.696365	1.524113	7.565212
H	2.632905	0.632500	7.308710
C	-0.510820	1.838408	6.956732
H	0.868833	1.792029	8.601284
H	-1.283247	2.355173	7.514878
H	-1.672734	1.748578	5.153022
C	3.811249	-2.889957	-1.138924
C	5.101800	-3.447947	-1.325265
C	5.290816	-4.561885	-2.152903
C	6.211719	-2.885954	-0.679582
C	6.555116	-5.095690	-2.326597
H	4.435066	-4.997067	-2.654620
C	7.649098	-4.532198	-1.683307
H	6.688757	-5.958017	-2.969824
C	7.471931	-3.427334	-0.861234

H	8.637987	-4.953478	-1.822602
H	8.322684	-2.983493	-0.356788
H	6.066781	-2.024457	-0.037547
C	1.623074	5.560450	-2.098042
C	2.751265	6.000906	-1.392318
C	1.117919	6.355505	-3.134567
C	3.352501	7.203288	-1.719602
H	3.142091	5.387216	-0.588375
C	2.844219	7.984806	-2.748620
H	4.224578	7.533286	-1.166575
C	1.726617	7.556352	-3.452628
H	3.318006	8.926281	-3.001499
H	1.326436	8.163111	-4.256946
H	0.246998	6.016489	-3.682280
C	-4.431985	-1.589130	-1.343687
C	-5.829183	-1.788128	-1.485353
C	-6.332690	-2.824228	-2.281680
C	-6.729539	-0.941513	-0.824856
C	-7.697976	-3.004931	-2.411547
H	-5.639671	-3.480823	-2.793686
C	-8.582571	-2.160931	-1.753419
H	-8.075475	-3.810749	-3.030676
C	-8.093161	-1.131059	-0.961232
H	-9.651624	-2.306103	-1.857517
H	-8.779666	-0.469932	-0.444668
H	-6.341220	-0.140797	-0.206277
H	-4.341656	0.940736	-3.197055
H	-3.549368	2.908649	-3.741703
H	-4.522612	-1.531866	3.715883
H	-2.591247	-0.736907	4.361621
H	-2.105147	-4.436313	-2.881248

H	-0.046449	-5.166781	-2.968148
H	4.706282	0.524072	-2.945306
H	3.757793	2.497490	-3.017091
H	4.022986	-3.593370	1.742056
H	3.651763	-3.280265	3.870998
H	0.268641	5.286271	3.159043
H	0.485573	5.476807	0.994236

$[PtH_2Cu_{11}\{S_2P(O^iPr)_2\}_6(CCPh)_3]$ (**3**)

Cu	-0.898602	-1.594827	2.022590
Cu	2.684019	-0.642734	0.399658
Cu	0.432798	2.072710	1.762063
Cu	-2.122418	-1.580891	-0.693915
Cu	1.262327	-0.597729	-2.282329
Cu	-1.184204	2.300896	-0.800330
Cu	1.478662	-0.236891	2.885378
Cu	-1.350931	0.162378	-2.659435
Cu	0.697878	-2.541779	-0.627534
Cu	1.759445	2.055125	-0.457359
Cu	-2.335251	0.492787	1.369815
S	-1.189696	-3.511870	-1.690576
S	-0.129955	-1.189617	-4.124116
S	0.315057	-3.564008	1.476192
S	3.205612	-1.788105	2.526785
S	2.173445	1.553470	-2.720240
S	-1.218990	2.444736	-3.214440
S	3.932936	1.430785	0.376411
S	2.202924	1.968287	3.411282
S	-3.452144	2.077518	-0.043292
S	-3.648008	-0.546989	-2.441721
S	-1.598299	2.024448	2.992259

S	-0.266068	-0.986615	4.231977
P	-0.865566	-2.988488	-3.604636
P	2.128918	-3.477291	2.349000
P	0.740486	2.664955	-3.602595
P	3.838856	2.137534	2.253516
P	-4.485173	0.837584	-1.253970
P	-1.229171	0.760532	4.510056
C	2.449093	-1.939076	-1.282185
C	3.689751	-1.940802	-1.291950
C	5.087375	-2.114019	-1.499867
C	5.537535	-2.719859	-2.680522
C	6.889991	-2.908051	-2.896881
C	7.815054	-2.499535	-1.944774
C	7.377953	-1.898925	-0.772619
C	6.026277	-1.704183	-0.548105
H	5.679251	-1.231857	0.362556
H	8.095892	-1.576896	-0.027011
H	7.225857	-3.375820	-3.815360
H	4.811348	-3.034708	-3.420137
C	0.410357	3.365134	0.168510
C	-0.298627	4.362620	-0.034817
C	-0.930789	5.631016	-0.171574
C	-0.306999	6.772976	0.349551
C	-0.902269	8.014360	0.221958
C	-2.125518	8.141594	-0.423595
C	-2.750665	7.016647	-0.942525
C	-2.162195	5.769848	-0.820817
H	-2.647855	4.888282	-1.221702
H	-3.706193	7.109998	-1.445919
H	-0.409980	8.889544	0.630665
H	0.645491	6.667574	0.854632

C	-2.847042	-1.405056	1.326877
C	-3.551244	-2.367951	0.980570
C	-4.475031	-3.445071	0.847682
C	-4.853662	-3.934837	-0.406271
C	-5.769239	-4.968050	-0.505049
C	-6.317242	-5.531773	0.638550
C	-5.945025	-5.054448	1.888624
C	-5.033441	-4.020285	1.997132
H	-4.421746	-3.491180	-1.295092
H	-6.056111	-5.337185	-1.483122
H	-6.368827	-5.491738	2.785560
H	-4.739486	-3.643580	2.969372
H	1.252197	0.203078	1.153103
H	-1.345678	0.077612	-0.907704
Pt	0.013079	0.016158	0.039324
H	-0.042366	-3.977671	-4.177871
H	-2.069294	-3.172638	-4.314878
H	2.935420	-4.434940	1.704671
H	1.996823	-4.030794	3.638765
H	1.080009	4.014974	-3.392056
H	0.914381	2.536880	-4.995764
H	4.178060	3.504065	2.205071
H	4.924267	1.598463	2.973946
H	-5.438891	0.191166	-0.444758
H	-5.300037	1.651799	-2.066770
H	-2.454919	0.479169	5.144588
H	-0.538903	1.469761	5.513783
H	8.874729	-2.648202	-2.117796
H	-2.590240	9.116099	-0.520682
H	-7.032025	-6.342602	0.556